Kinetics and Thermodynamics of Protein Adsorption: A Generalized Molecular Theoretical Approach

Fang Fang and Igal Szleifer

Department of Chemistry, Purdue University, West Lafayette, Indiana 47907 USA

ABSTRACT   The thermodynamics and kinetics of protein adsorption are studied using a molecular theoretical approach. The cases studied include competitive adsorption from mixtures and the effect of conformational changes upon adsorption. The kinetic theory is based on a generalized diffusion equation in which the driving force for motion is the gradient of chemical potentials of the proteins. The time-dependent chemical potentials, as well as the equilibrium behavior of the system, are obtained using a molecular mean-field theory. The theory provides, within the same theoretical formulation, the diffusion and the kinetic (activated) controlled regimes. By separation of ideal and nonideal contributions to the chemical potential, the equation of motion shows a purely diffusive part and the motion of the particles in the potential of mean force resulting from the intermolecular interactions. The theory enables the calculation of the time-dependent surface coverage of proteins, the dynamic surface tension, and the structure of the adsorbed layer in contact with the approaching proteins. For the case of competitive adsorption from a solution containing a mixture of large and small proteins, a variety of different adsorption patterns are observed depending upon the bulk composition, the strength of the interaction between the particles, and the surface and size of the proteins. It is found that the experimentally observed Vroman sequence is predicted in the case that the bulk solution is at a composition with an excess of the small protein, and that the interaction between the large protein and the surface is much larger than that of the smaller protein. The effect of surface conformational changes of the adsorbed proteins in the time-dependent adsorption is studied in detail. The theory predicts regimes of constant density and dynamic surface tension that are long lived but are only intermediates before the final approach to equilibrium. The implications of the findings to the interpretation of experimental observations is discussed.

INTRODUCTION

Protein adsorption plays a major role in a variety of important technological and biological processes (Clerc and Lukosz, 1997; Denizli et al., 2000; Ghose and Chase, 2000; Hlady and Buijs, 1996; Montdargent and Letourneur, 2000; Shi and Ratner, 2000; Slomkowski, 1998; Topoglidis et al., 1998). For example, blood proteins tend to adsorb into surfaces of foreign materials. This is the first step on surface-induced thrombosis (Andrade and Hlady, 1986; Horbett, 1993; E. F. and S. 1993; Tanaka et al. 2000). A large number of biotechnological devices include surface-bound proteins, e.g., biosensors (Nyquist et al., 2000; Slomkowski et al., 1996; Sukhishvili and Granick, 1999; Zhou et al., 2000). Separation of proteins by chromatography involves the competitive adsorption of the particles (Wang 1993). The understanding of the fundamental factors that determine protein adsorption are imperative to improve our ability to design biocompatible materials and biotechnological devices. Moreover, protein adsorption is a very important fundamental problem that involves large competing energy scales and conformational statistics that may result in reversible and irreversible processes.

The adsorption of proteins on surfaces is a complex process. The adsorbing particles are large, and, thus, the surface–protein interactions are usually long range and the strength is many times the thermal energy. Further, due to the large size and the shape of the particles, the interactions between the adsorbed particles on the surface are nontrivial and can be strongly influentiated by the fact that the particles may undergo conformational changes upon adsorption (Billsten et al., 1995; Ishihara et al., 1998; Kondo and Fukuda, 1998; Nasir and McGuire, 1998; Norde and Giacomelli, 1999, 2000; Tan and Martic, 1990; Van Tassel et al., 1998; Gidalevitz et al., 1999). Actually, the kinetics and thermodynamics of protein conformational changes on the surface is a very complex subject and their understanding is at its early stages. The idea behind the work presented here is an attempt to formulate a molecular theoretical approach that can be applied to study both the equilibrium and the kinetic behavior of protein adsorption.

On experimental studies (Green et al., 1999; Malmsten, 1997), it has been observed that, when two or more kinds of proteins are present in solution, such as in blood plasma, the adsorption is the result of the competition between the time scale to reach the surface and the strength of the surface–protein interaction. For example, in blood plasma solutions of albumin, immunoglobulin-G (IgG) and fibrinogen (Fgn) in contact with a polystyrene surface, the initial adsorption is dominated by the smaller protein (albumin), which are also at larger concentrations in the bulk, to be later replaced by the larger proteins like IgG and Fgn. This sequential adsorption is called the Vroman sequence. In other experi-

ments (Lassen and Malmsten, 1997), different adsorption patterns are observed when the surfaces are changed. On the hydrophobic PP-HMDSO (hexamethyldisiloxane), surface albumin and IgG dominate the adsorption. However, on hydrophilic PP-DACH (1,2-diaminocyclohexane) and PP-AA (acrylic acid) surfaces, Fgn is almost exclusively found on the surface. These experimental observations demonstrate that the incorporation of the solution conditions and the protein–surface interactions have to be considered for the proper understanding and description of the adsorption process.

One of the most important contributions to the understanding of the kinetics of protein adsorption is the random sequential adsorption (RSA) model (Feder and Giaever, 1980; Schaaf and Talbot, 1989). In this approach, the proteins are assumed to be rigid particles that interact only through excluded volume interactions. The particles are assumed to irreversibly adsorb to the surface, and, thus, they do not have translational degrees of freedom or desorption on the surface. This model has been very useful in understanding why the kinetics of protein adsorption do not follow the Langmuir predictions. Furthermore, the model has been extended to consider conformational changes, desorption, and the treatment of mixtures (Van Tassel et al., 1994, 1996, 1998). The main limitation of this model is that it is hard to include detailed molecular information of the proteins and the formulation is based on a kinetic approach.

Some other studies have assumed that the adsorption kinetics is determined by the diffusion of the proteins to the surface (Iordanskii et al., 1996), whereas others assume that the dominant regime is the one controlled by a kinetic (activated) process (Chatelier and Minton, 1996; Minton, 1999). In a recent study, Cho et al. (1997) formulated a model in which both the diffusion and kinetic processes were included. Olson and Talbot (2000) studied the equilibrium and kinetics of adsorption of a polydisperse mixture. Each of these models has provided important insights toward the understanding of the adsorption process. However, none of them can describe both the equilibrium and kinetics of the adsorption process within the same molecular approach that can be applied for a large variety of experimental systems.

The theory that we use in this paper is based on the formulation of the free energy of the system. The minimization of the free energy provides the equilibrium state of the system, and, thus, we can study the protein adsorption isotherms. Furthermore, the free energy formulation enables the study of possible conformational changes of the protein on the surface. The equilibrium version of the theory for protein adsorption was originally formulated to study the ability of grafted polymer layers to prevent, or reduce, protein adsorption (Szleifer, 1997b). The predictions of the theory were shown to be in excellent quantitative agreement with experimental observations for the equilibrium adsorption isotherms of lysozyme on surfaces with grafted poly-

ethylene oxide layers (McPherson et al., 1998; Satulovsky et al., 2000). The theory was later generalized to study the kinetics of the adsorption process in the same systems (Satulovsky et al., 2000). The basic idea in the dynamic version of the theory is to start with an equilibrium bulk system that, at time zero, is put in contact with a surface. The presence of the surface induces a distance dependent chemical potential of the proteins. The free energy of the new system is formulated, but instead of minimizing to obtain the new equilibrium state in the presence of the surface, the time evolution of the density of proteins is evolved with a diffusion-like equation, with the driving force being the gradient of chemical potentials arising from the sudden presence of the surface. These chemical potentials are obtained as derivatives of the time-dependent free energy with respect to the local density of proteins. Similar approaches were used for the adsorption of surfactants (Diamant and Andelman, 1996) and polymers (Fraaije, 1993; Hasegawa and Doi, 1997). Recently, it has been shown that this kind of dynamic equations can be derived for the time dependence of the density from density functional theory (Marconi and Tarazona, 1999).

In this paper, we are interested in using the same theoretical approach but to the study of protein adsorption on bare surfaces. The idea is to understand what are the parameters that determine the different dynamic regimes. Further, we are interested in studying in detail the effect of conformational changes on the kinetics of adsorption and also the adsorption of proteins mixtures.

The paper is organized as follows: the next section contains a description of the theoretical methodology, including a detailed presentation of the way the equations are solved. The following section present a variety of representative results. Finally, the last section includes our conclusions.

THEORETICAL APPROACH

In this section, we present our theoretical approach to study the equilibrium and kinetic properties of the adsorption of proteins to planar surfaces. We will present a general theoretical framework for the determination of equilibrium adsorption isotherms in the case of protein mixtures. The treatment explicitly includes the possibility that the proteins have many different configurations. The second part of this section presents the dynamic theory that we use to study the kinetics of protein adsorption.

After the presentation of the general thermodynamic and kinetic approaches, we will show the specific cases for which we present explicit calculations below. Namely, the adsorption of proteins that are assumed to have a single configuration in the bulk but that can undergo conformational changes upon contact with the surface and those assumed to be a mixture of proteins of different sizes for a variety of different bulk conditions and surfaces. Following

the model, we present details on the numerical methodology used in solving the equilibrium and kinetic equations.

Equilibrium free energy

Consider a surface of total area A in contact with a protein solution, Fig. 1. The solution is composed by a mixture of proteins characterized by a bulk chemical potential $\mu_{i,bulk}^{pro}$, with i denoting the type of protein. Equivalently, we can represent the properties of the protein solution by the density of molecules $\rho_{i,bulk}^{pro}$. Each protein can be in any of its possible configurations. We denote the set of configurations of protein of type i by $\{\gamma_i\}$. Let us define by $P(\gamma_i; z)$ the probability distribution function (pdf) of proteins of type i to be in configuration γ_i at distance z from the interface. The pdf can also be thought as the conditional probability that a protein of type i at distance z from the surface is in conformation γ_i.

The relevant surface free energy density (per unit area) of the system (Rowlinson and Widom, 1982), assuming inhomogeneities in density only in the direction perpendicular to the surface, z, is given by
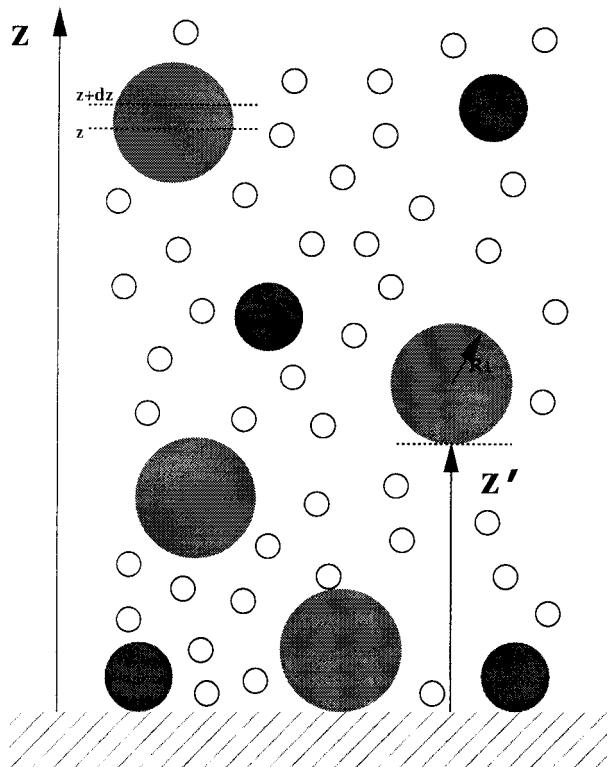

FIGURE 1 Schematic representation of the system containing a mixture of proteins dissolved in a low-molecular-weight solvent in contact with a surface. The filled circles are protein molecules with different sizes and the empty circles are solvent molecules. The z direction is defined perpendicular to the surface. The protein at position z' represents the molecules with their point of shortest distance with the surface being z'.

$$\frac{\beta W}{A} = \sum_i \left\{ \int \rho_i^{pro}(z) \left[\ln[\rho_i^{pro}(z)v_s] \right. \right.$$

$$+ \sum_{\{\gamma_i\}} P(\gamma_i; z)[\ln P(\gamma_i; z) + \beta U_{int}(\gamma_i) + \beta U_{ps}(\gamma_i; z)]$$

$$+ \sum_j \sum_{\{\gamma_j\}} \frac{1}{2} \int \beta \chi_{\gamma_i \gamma_j}(|z - z'|) \rho_j^{pro}(z') P(\gamma_j; z') dz'$$

$$\left. - \beta \mu_{i,bulk}^{pro} \right] dz \left. \right\}$$

$$+ \int \frac{\phi_s(z)}{v_s} [\ln \phi_s(z) - \beta \mu_s] \, dz, \quad (1)$$

where the first and second terms represent the z-dependent translational (mixing) and the conformational entropy of the proteins, respectively. The third term is the intramolecular energy of the proteins. The fourth term includes the average interaction between the protein at z with the surface, $U_{ps}(\gamma_i; z)$ is the interaction between the protein i in configuration γ_i with the surface. The fifth term is the protein–protein attractive interactions. $\chi_{\gamma_i \gamma_j}(|z - z'|)$ represents the strength of the interactions between protein in configuration γ_i at z and protein in configuration γ_j at z'. The sixth term is the chemical potential term necessary because we consider the surface in equilibrium with a bulk solution, i.e., the surface is in contact with a bath of proteins. The last two terms represent the solvent contribution, which include the translational (mixing) entropy and the chemical potential terms. $\phi_s(z)$ and μ_s represent the volume fraction at z and the chemical potential of the solvent molecules, respectively. Note that the argument of the first ln term in Eq. 1 contains the volume of the solvent to make the product dimensionless. Further, we will use v_s as the unit of volume throughout.

Inspection of Eq. 1 shows that the repulsions between the molecules are not included in the free energy expression. These interactions are accounted for by packing constraints. Namely, for each distance z from the surface, the volume available between z and $z + dz$ is filled by the proteins or the solvent molecules. Thus, the volume constraint equation reads

$$\int \left[\sum_i \rho_i^{pro}(z') \sum_{\{\gamma_i\}} P(\gamma_i; z') v(\gamma_i; z', z) \right] dz' + \phi_s(z) = 1$$

$$\text{for all } z, \quad (2)$$

where the first term represents the volume fraction that the proteins occupy at z, and the second term is the volume fraction of solvent. Note that the volume fraction of proteins includes the sum over all the molecules at different dis-

tances from the surface (z') that contribute volume to z. $v(\gamma_i; z', z) \, dz'$ is the volume that the protein in configuration γ_i at z' occupies at z.

The next step is to determine the density of proteins and solvent as a function of z and the pdf of protein configurations. The systems free energy is a functional of $\rho_i^{pro}(z)$, $\phi_s(z)$, $P(\gamma_i; z)$. These quantities are found by minimization of the systems free energy, Eq. 1, subject to the packing constraints, Eq. 2. The minimization is carried out introducing a set of Lagrange multipliers, $\beta\pi(z)$, to yield for the pdf of the protein configurations

$$P(\gamma_i; z) = \frac{1}{q_i(z)} \exp\left[-\beta U_{int}(\gamma_i) - \beta U_{ps}(\gamma_i; z) \right.$$

$$- \int \beta\pi(z')v(\gamma_i; z, z') \, dz'$$

$$\left. - \sum_j \sum_{\{\gamma_j\}} \int \beta\chi_{\gamma_i\gamma_j}(|z - z'|)\rho_j^{pro}(z')P(\gamma_j; z') \, dz' \right], \quad (3)$$

where $q_i(z)$ is the normalization constant that ensures for each z that $\sum P(\gamma_i; z) = 1$. The partition function is given by the sum over all the configurations of the exponential term in Eq. 3.

The density profile of proteins of type i is

$$\rho_i^{pro}(z)v_s = q_i(z)\exp[\beta\mu_{i,bulk}^{pro}], \quad (4)$$

and, for the solvent volume fraction, we have

$$\phi_s(z) = \exp[-\beta\pi(z)v_s + \beta\mu_s]. \quad (5)$$

The only unknowns are the Lagrange multipliers, which are obtained by replacing the explicit expressions for the pdf and density profiles, Eqs. 3, 4, and 5, into the constraint equation, Eq. 2. The explicit form of the equations solved will be described below for the specific model systems that we present in the Results section. The physical meaning of the Lagrange multipliers can be understood by looking at the expression for the solvent density profile, Eq. 5. Writing this expression in the form,

$$\beta\mu_s = \ln \phi_s(z) + \beta\pi(z)v_s, \quad (6)$$

shows that the Lagrange multipliers are related to the (z-dependent) osmotic pressure necessary to keep the chemical potential of the solvent constant at all z.

The expressions for the density profiles and the pdf of the proteins enable us to understand what are the factors determining the equilibrium amount of protein adsorbed and the optimal adsorbed conformations. The partition of proteins as a function of the distance from the surface is determined by the thermodynamic equilibrium condition of constant chemical potential at all z. Thus, we can write Eq. 4 in the form

$$\beta\mu_{i,bulk}^{pro} = \ln \frac{\rho_i^{pro}(z)v_s}{q_i(z)}, \quad (7)$$

which requires the chemical potential of the proteins at all z to be that of the bath, i.e., the value given by the bulk solution. The amount of protein of type i on the surface ($z = 0$) is determined by the value of the partition function on the surface, $q_i(0)$. Thus, the partition function and the density at the surface, through Eq. 7, will be determined by the interplay between the interactions that increase the value of the partition function and those that reduce it. The attractive components (which increase $q_i(0)$) are the bare surface–protein interaction and the protein–protein van der Walls attractions. The repulsions (which decrease $q_i(0)$) are those determined by the pressure–volume-like term (PV), given by the product of the lateral pressures $\pi(z)$ by the volume of the protein as a function of z. This repulsive term is associated with the PV work necessary to bring the protein from the bulk solution to the surface. Thus, it is not enough to have a strong attractive interaction with the surface for a protein to preferentially adsorb, its volume distribution should be such that the repulsions are not too large. The same type of argument is obtained to explain the preferential adsorption of a given conformation. To this end, it is convenient to define the density of proteins at z in conformation γ_i, by multiplying the pdf of that conformation, Eq. 3, by the density of proteins of type i at z, Eq. 4, to obtain

$$\rho_{\gamma_i}^{pro}(z)v_s = [\rho_i^{pro}(z)v_s]P(\gamma_i; z)$$

$$= \exp[\beta\mu_{i,bulk}^{pro}]\exp[-\beta U_{int}(\gamma_i) - \beta U_{ps}(\gamma_i; z)$$

$$- \int \beta\pi(z')v(\gamma_i; z, z') \, dz'$$

$$- \sum_j \sum_{\{\gamma_j\}} \int \beta\chi_{\gamma_i\gamma_j}(|z - z'|)\rho_j^{pro}(z')P(\gamma_j; z') \, dz'. \quad (8)$$

This expression shows that the condition of equal chemical potential at all z has to be fulfilled for each protein configuration. Further, note that the value of constant chemical potential for each configuration is that of the bulk protein.

We can rewrite the equilibrium condition for each protein conformation in the form

$$\beta\mu_{i,bulk}^{pro} = \ln[\rho_{\gamma_i}^{pro}(z)v_s] + \beta U_{mf}(\gamma_i, z), \quad (9)$$

where

$$U_{mf}(\gamma_i; z) = U_{int}(\gamma_i) + U_{ps}(\gamma_i; z)$$

$$+ \int \pi(z')v(\gamma_i; z, z') \, dz'$$

$$+ \sum_j \sum_{\{\gamma_j\}} \int \chi_{\gamma_i\gamma_j}(|z - z'|)\rho_j^{pro}(z')P(\gamma_j; z') \, dz', \quad (10)$$

is the potential of mean force (Chandler, 1987) between the protein, in conformation γ_i at distance z, and the surface. Namely, it is the work required to bring the protein in conformation γ_i from the bulk to the distance z from the surface. This way of writing the chemical potential enables the understanding of the factors that determine the type of conformation and protein that adsorbs on the surface, and it will be useful in the kinetic description presented in the next section. Note that the potential of mean force, and the last term in the solvent chemical potential Eq. 6, are the excess (or nonideal) contributions to the chemical potential.

Using the definition of the potential of mean force, we can see that the requirement of constant chemical potential, and thus what determines the amount of proteins in each conformation that are adsorbed, depends on the cost (or gain) of bringing a protein from the bulk solution to contact with the surface. There are four contributions that determine the potential of mean force. 1) The internal energy of the conformation. This term is independent of z. 2) The bare surface–protein interaction. This is usually a strongly attractive term. 3) The intermolecular repulsive interaction term. This term becomes more prominent as the density increases and therefore favors small densities at the surface. 4) The intermolecular attractive term, which favors large densities. The interplay between these contributions will determine the amount and type of conformation that will adsorb on the surface. Further, the manipulation of these contributions may lead to an enhanced (or decreased) adsorption and thus control of the amount and type of protein adsorbed (Szleifer, 1997a).

In the Results section, we will show explicit examples for how the interplay between the different interactions determines the optimal protein and conformation adsorbed. Further, we will discuss how this understanding can lead to the design of surfaces or conditions for optimal adsorption.

Equations of motion

We now treat the process of how the proteins in solution adsorb into the surface. Consider a solution containing a mixture of proteins at bulk densities $\rho_{i,\text{bulk}}^{\text{pro}}$ (or equivalently chemical potential $\mu_{i,\text{bulk}}^{\text{pro}}$) dissolved in a low molecular-weight solvent. This homogeneous solution is in equilibrium, and, at time $t = 0$, is brought in contact with a layer of pure solvent that is in contact with a surface on the other end. The direction perpendicular to the surface is denoted as the z direction. A schematic view of the system is shown in Fig. 1.

The contact between the pure solvent and the protein solution induces the diffusion of the proteins toward the pure solvent. Further, the sudden presence of the surface implies that the proteins now feel an anisotropic interaction due to the bare protein–surface attractions. Therefore, the chemical potential of the proteins closer to the surface is not the same as that of the proteins in the bulk (far from the

surface). The nonconstant chemical potential of the proteins as a function of z is the driving force for mass transport. Further, the protein–surface interaction and the motion toward the surface will depend upon the conformation of the protein.

The time evolution of the density of proteins of type i in conformation γ_i at distance z from the surface, $\rho_{\gamma_i}^{\text{pro}}(z, t)$, contains two contributions. The first one is the transport of the same conformation from neighboring distances. The second is from conformational changes of proteins at distance z from the surface. The transport can be described with a generalized diffusion equation, and the conformational changes can be written as kinetic master equations. The result is

$$\frac{\partial \rho_{\gamma_i}^{\text{pro}}(z, t)}{\partial t} = D_{\gamma_i} \frac{\partial}{\partial z}\left[\rho_{\gamma_i}^{\text{pro}}(z; t)\frac{\partial \beta \mu_{\gamma_i}^{\text{pro}}(z; t)}{\partial z}\right]$$
$$+ \sum_{\gamma_i'}[k(\gamma_i' \rightarrow \gamma_i)\Phi(\gamma_i' \rightarrow \gamma_i; z)\rho_{\gamma_i'}^{\text{pro}}(z, t)$$
$$- k(\gamma_i \rightarrow \gamma_i')\Phi(\gamma_i \rightarrow \gamma_i'; z)\rho_{\gamma_i}^{\text{pro}}(z, t)], \quad (11)$$

where the first term represents the mass transport. D_{γ_i} is the diffusion coefficient of proteins of type i in conformation γ_i, which is assumed to be composition independent; $\mu_{\gamma_i}^{\text{pro}}(z; t)$ is the time-dependent chemical potential, defined as an extension of the equilibrium quantity. Namely, we define

$$\mu_{\gamma_i}^{\text{pro}}(z; t) = \frac{\delta(W/A)}{\delta \rho_{\gamma_i}^{\text{pro}}(z, t)}, \quad (12)$$

where W/A is the time-dependent free energy per unit area of the system. For the time-dependent free energy, we use the same expression as the equilibrium quantity, but the protein densities are not the ones that minimize the free energy but are given by the values obtained by the time-evolution equation.

The last two terms in the kinetic equation, Eq. 11, represent the time-dependent conformational changes. There is a gain and a loss term. The gain term arises from all the conformations γ_i' that can undergo a conformational change to configuration γ_i. The last term represents the conformational change from γ_i to any possible configuration. The constants $k(\gamma_i' \rightarrow \gamma_i)$ represent the intrinsic rate of conformational change of the protein from γ_i' to γ_i. Namely, it is the rate associated with the conformational change of the protein in the presence of pure solvent. The factor $\Phi(\gamma_i' \rightarrow \gamma_i; z)$ represents the effect of the intermolecular and surface interactions to the rate of conformational change from γ_i' to γ_i. This term can be interpreted as the probability of finding the necessary space for the conformation to change from γ_i' to γ_i, modulated by the appropriate energetic gain or loss. This probability is related to the work necessary to change the conformation in the given environment. In the terms defined in the previous section, this quantity will be the Boltzmann factor of the interaction difference between the

two conformations in the given environment at z and t. This quantity is readily obtained from the theory by using the third term in Eq. 10 with the temporal densities obtained from the dynamic equations. Note that this term will depend very strongly on the density distribution, and, therefore, will be a function of time. We will show some explicit examples below.

The boundary conditions to solve the dynamics equation is that the gradient of chemical potential at the surface (and in the bulk solution) is zero. Namely,

$$\left[\frac{\partial \beta \mu_{\gamma_i}^{pro}(z; t)}{\partial z}\right]_{z=0, z=\infty} = 0. \quad (13)$$

This boundary condition at $z = 0$ is, in reality, the condition that the molecules cannot diffuse behind the surface, i.e., to negative values of z.

At this point, it is important to emphasize the difficulties associated with treating realistic proteins. Eq. 11 requires the knowledge of the rate of change of the protein conformations from one to another. This is a formidable task, considering the fact that even the conformational space of real proteins cannot be properly sampled with the techniques and computer resources available today (Chan and Dill, 1998; Scheraga, 1996; Yue et al., 1995; Brooks et al., 1998). Thus, we need to use simplified models. However, these simplified models are based on the behavior of real proteins. For example, in many cases, proteins in bulk exist in a small set of conformations that are close to the native structure. Thus, the description of a single conformation of the protein in bulk is a reasonable approximation. There is clear experimental evidence that proteins undergo conformational changes upon adsorption on surfaces and interfaces (Billsten et al., 1995; Ishihara et al., 1998; Kondo and Fukuda, 1998; Nasir and McGuire, 1998; Norde and Giacomelli, 1999, 2000; Gidalevitz et al., 1999; Tan and Martic, 1990; Van Tassel et al., 1998). There are two kinds of configurational changes that can happen upon adsorption. One of them corresponds to the denaturation of the protein from the native configuration to a random coil. In the second, the protein undergoes a conformational change to a very small subset of conformations that are as unique as the native configuration but with a different structure. Recent extensive calculations in a simple model system strongly suggests that the second one is the most common case for solid surfaces (R. Abdulla, Jr. and I. Szleifer, manuscript in preparation). The calculations presented below correspond to this second case. It is important to emphasize that the rate constants and the protein conformations are input to the theory. Thus, even in the case of multiple adsorbed configurations, if those data are available, the kinetic theory can be applied without any major additional complications.

To understand the time-dependent adsorption, it is useful to look at each of the contributions separately. We start with the mass transport part. The driving force for this motion is the gradient in (time-dependent) chemical potentials. We can use the analog of Eq. 9 for the time-dependent chemical potential to obtain

$$\beta \mu_{\gamma_i}^{pro}(z; t) = \frac{\delta(\beta W/A)}{\delta \rho_{\gamma_i}^{pro}(z, t)}$$

$$= \ln[\rho_{\gamma_i}^{pro}(z, t) v_s] + \beta U_{mf}(\gamma_i; z; t). \quad (14)$$

Replacing this expression into the transport part of the equation of motion, we obtain

$$\frac{\partial \rho_{\gamma_i}^{pro}(z, t)}{\partial t} = D_{\gamma_i}\left[\frac{\partial^2 \rho_{\gamma_i}^{pro}(z; t)}{\partial z^2} + \frac{\partial}{\partial z}\left(\rho_{\gamma_i}^{pro}(z; t)\frac{\partial \beta U_{mf}(\gamma_i; z; t)}{\partial z}\right)\right]. \quad (15)$$

The first term in the rhs of the equation is the regular diffusion term and it arises from the ideal term in the free energy. The fact that we explicitly consider the interactions between the molecules and between the proteins and the surface results in the additional term to the transport equation. Thus, the motion of the proteins is driven by the effective interactions between the particles and the surface. The time scale for the diffusion process will depend on the explicit form of the potential of mean force, $U_{mf}(\gamma_i; z; t)$. As we will show, this quantity undergoes dramatic changes as a function of time, and, thus, the adsorption process changes character.

Throughout the discussion in the Results section, we refer to two distinct dynamic regimes. We call them diffusion-controlled regime and kinetic (or activated) regime. The diffusion-controlled regime refers to the dynamic processes that are dominated by the first term in the rhs of Eq. 15. This will be the "ideal" diffusion driven exclusively by the gradient of densities. We also include in this regime the "driven" diffusion, which represents the motion that arises from the bare surface–protein interactions. The kinetic or activated regime is the one dominated by the nonideal contribution to the chemical potential arising from the intermolecular interactions. This term contains in it any kinetic barriers that appear in the system due to the repulsive interactions between molecules.

At this point, it is important to emphasize one of the main differences between our approach and the purely kinetic approaches that can be found in the literature. Even for the pure transport process, our theory describes the adsorption and desorption process at once. We do not need to include an explicit term that considers the possibility of desorption. Furthermore, according to our theory, there is only one elementary time scale measured by the diffusion constant. The different time scales for adsorption and desorption will depend upon the time and z dependence of the potential of mean force. Further, our approach warrants the approach to equilibrium. However, some types of irreversible adsorption

can also be treated within the same framework, because, in that case, the time scale of the adsorption process will be slow in the experimental time scale.

It should be noted that, although we have emphasized the advantages of our approach, there are many limitations as well. The main one that we comment upon here is that the lateral dynamics (within a given z) are assumed to be instantaneous as compared to the diffusion to the surface, Namely $\rho(x, y, z; t) = \rho(z; t)$ for all x, y. Although recent Brownian dynamic simulations have shown that this is a reasonable approximation (Ravichandran and Talbot, 2000), it is important to keep its limitation in sight. Additional important limitations will be discussed in the Conclusions section.

The second contribution to the time-dependent adsorption, see Eq. 11, arises from the ability of the molecules to undergo conformational changes. As mentioned above, this is a rather complex and yet barely understood process. Thus, we will use a simple model to understand the effect of conformational changes on the kinetics of adsorption. This will be the case in which the conformational change can only occur upon contact of the protein with the surface.

Eq. 11 shows the need to provide the rate constants for conformational transformations $\gamma \rightarrow \gamma'$ and $\gamma' \rightarrow \gamma$. However, because the system will reach thermodynamic equilibrium, only one is needed. The ratio of the rate constants is proportional to the product of the ratio of the conformation populations and the ratio of the repulsive factors at equilibrium.

In the next subsection, we describe in detail the model systems that we will study and the parameters used in the calculations. Further, we present the explicit sets of equations that we solve and the numerical methodology used.

Model systems

We consider a set of simple systems to apply the theory developed above for the study of the thermodynamic and kinetic properties of protein adsorption. We study two different kinds of systems. The first is a binary mixture of model proteins. Both proteins are modeled as spherical in shape and they differ in size and in their interactions with the surface. These proteins can exist in a single configuration even when they are adsorbed on the surface. The motivation to study this mixture is to understand competitive adsorption in which the proteins differ in size and surface interaction. Namely, we want to understand the underlying physical process that is responsible for the Vroman sequence (Green et al., 1999). Further, we are interested in the general properties of competitive adsorption and under what condition one should expect adsorption of one or the other species. Thus, we chose a model that contains the minimal ingredients to study these effects, without too many complications that may cloud the physical origin of the observed behavior.

The mixtures are composed by two protein-like particles. Because both particles can exist in only one configuration, we take $U_{int}(\gamma_i) = 0$. The larger particle is the same size as our previous model for lysozyme (McPherson et al., 1998). Namely, it is a particle with a radius of 15 Å. The potential of interaction between this protein and the surface is shown in Fig. 2. The distance dependence of the protein–surface interaction is taken from the atomistic calculations of the interactions between lysozyme and hydrophobic surfaces as calculated by Lee and Park (1994). However, the strength of the attraction is taken to be $\frac{1}{3}$ of the original calculated one. The reason for this choice is that the extensive kinetic calculations that will be shown in the next subsection are less computationally demanding for a weaker potential. Furthermore, we have found that the predictions of the kinetic and thermodynamic behavior is qualitatively the same, and, therefore, we can perform more systematic studies with the weaker attractive potential.

The small particle has a radius that is $\frac{3}{5}$ that of the large protein. The distance dependence of the attractive interaction between the surface and the small protein is the same as that shown in Fig. 2. However, we vary the strength of the attraction in a wide range of values, as will be explicitly shown in the Results section. We assume that the solvent is equally good to both proteins. Thus, we model the intermolecular, protein–protein and protein–solvent interactions as purely repulsive. Namely, $\chi_{\gamma_i\gamma_j} = 0$ for all $\gamma_i\gamma_j$.

Some comments are needed here. The choice of purely repulsive interactions implies that all the attractive intermolecular interactions are the same and not that they are absent in the system. One can question the validity of this approximation merely on the basis of colloidal interactions, where it is known that the strength of the attractive interactions between particles is a function of the size of the particles
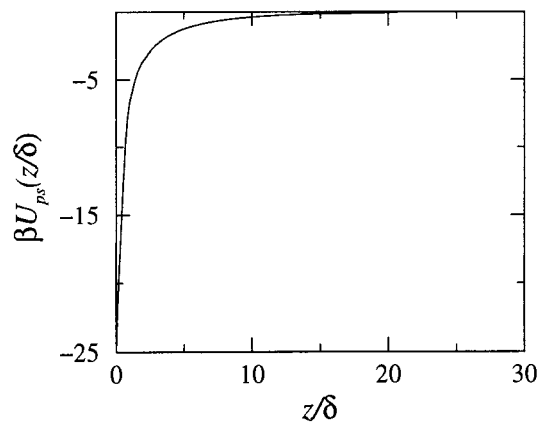

FIGURE 2 The distance dependence of the attractive interaction between one large protein particle and the surface in a binary mixture of model proteins. The interactions are measured in units of $\beta = 1/kT$, the distances are measured in units of $\delta = D/5$, where D is the diameter of the largest protein that we model.

(Israelachvili, 1991). We have carried out some calculations for both the kinetic and the thermodynamic properties of mixtures of model proteins where the attractive interaction was explicitly considered. We found that, unless we are close to a phase separation region, i.e., the two-phase region where the mixture separates into two solutions with different miscibilities for the proteins, the qualitative results are very similar to the ones obtained for the athermal (good solvent) systems. Therefore, we decided to concentrate our attention on these simpler systems.

The equations necessary to study the kinetic and thermodynamic behavior of the mixtures just defined are obtained from the general equations derived above. Because there are no conformational changes, only the densities of the proteins as a function of the distance from the surface (and time) are relevant quantities. The density of particles of type i at equilibrium is given by

$$\rho_i^{pro}(z)v_s = \exp[\beta\mu_{i,bulk}^{pro}]\exp\left[-\beta U_{ps}^i(z)\right.$$
$$\left.-\int_z^{z+2R_i}\beta\pi(z')v_i(z, z')\,dz'\right], \quad (16)$$

where $v_i(z, z')\,dz'$ is the volume that the protein (sphere) of type i, with its point of closest distance to the surface at z, occupies at z', and $U_{ps}^i(z)$ is the attraction between the surface and the protein (sphere) of type i shown in Fig. 2 or its appropriate modification (see above). R_i is the radius of the protein of type i. To determine the Lagrange multipliers, $\beta\pi(z')$, we need to solve the constraint equations, which for the binary mixture considered here, is (see Eq. 2)

$$\int_{z-2R_1}^z \rho_1^{pro}(z')v_1(z',z)\,dz'$$
$$+\int_{z-2R_2}^z \rho_2^{pro}(z')v_2(z', z)\,dz' + \phi_s(z) = 1$$

$$\text{for all } z, \quad (17)$$

which is solved by replacing Eq. 16 for each density and then by discretization of the z direction into finite elements. The volumes $v_i(z', z)\,dz'$ are given by the cross-sectional area of the sphere at z when the bottom of the sphere is at z'. Namely, $v_i(z', z)\,dz' = \pi\{R_i^2 - [R_i - (z' - z)]^2\}\,dz'$. The discrete version is obtained by integrating the cross-sectional area over the thickness of the discrete layer. The solution of these equations is straightforward, and, from them, we obtain the equilibrium adsorption isotherms. The bulk conditions of the solution are introduced in the chemical potentials, $\mu_{i,bulk}^{pro}$, which are explicitly given by

$$\beta\mu_{i,bulk}^{pro} = \ln[\rho_{i,bulk}^{pro}v_s] - \frac{V_i^{pro}}{v_s}\ln\phi_s^{bulk}, \quad (18)$$

where V_i^{pro} is the total volume of the protein and ϕ_s^{bulk} is the bulk volume fraction of the solvent. Eq. 18 is obtained from Eq. 16 by considering $\beta\pi(z)v_s = \beta\pi_{bulk}v_s = -\ln\phi_s^{bulk}$ and $U_{ps}^i(bulk) = 0$.

It should be noted that, due to the volume-constraint equations, we have reduced the number of independent thermodynamic variables by one. Namely, we cannot vary the volume of the system at a fixed number of proteins and solvent molecules. Therefore, we do not have absolute chemical potentials, but the chemical potential of the protein is, in reality, an exchange chemical potential that measures the work related with changing V_i^{pro}/v_s solvent molecules by one protein molecule of type i. Although we do not explicitly write the chemical potentials as exchanges, it should be clear that this is the quantity that we are calculating throughout this work. Further, for the same reason, the value of the chemical potential of the solvent is not a relevant quantity and therefore is not needed (Carignano and Szleifer, 1994), or, in other words, the chemical potentials of the proteins and the lateral pressures are measured with respect to the solvent chemical potential.

For the kinetic equations, we can write for protein of type i,

$$\frac{\partial\rho_i^{pro}(z, t)}{\partial t} = D_i \frac{\partial}{\partial z}\left[\rho_i^{pro}(z; t)\frac{\partial\beta\mu_i^{pro}(z; t)}{\partial z}\right], \quad (19)$$

where the time-dependent chemical potential is given by

$$\beta\mu_i^{pro}(z; t) = \ln[\rho_i^{pro}(z; t)v_s] + \beta U_{ps}^i(z)$$
$$+\int_z^{z+2R_i}\beta\pi(z'; t)v_i(z, z')\,dz', \quad (20)$$

and the time-dependent Lagrange multipliers are obtained from the time-dependent constraint equation,

$$\int_{z-2R_1}^z \rho_1^{pro}(z'; t)v_1(z', z)\,dz'$$
$$+\int_{z-2R_2}^z \rho_2^{pro}(z'; t)v_2(z', z)\,dz' + \exp[-\beta\pi(z; t)v_s] = 1$$

$$\text{for all } z. \quad (21)$$

The procedure to integrate the equations of motion, Eq. 19, is to start with the initial condition of a homogeneous (very low, $\rho = 10^{-10}$) density for $z \leq L$, and, for $z > L$, the proteins are at bulk density and do not change that density over time. This is to represent a flow cell (Calonder and Van Tassel, 2001). At $t = 0$, the surface–protein interactions are turned on. Then, using Eq. 20 for each protein, one obtains

the chemical potential profiles that are needed for a time iteration of the densities. After the densities for the new time are obtained, Eq. 21 is used for the time-dependent Lagrange multipliers so that the new chemical potentials can be obtained to perform the next time iteration. This procedure is continued until all the chemical potentials are the same, which corresponds to the new equilibrium condition.

The very low density used in the closed vicinity of the surface, instead of pure solvent, is for numerical convenience. Further, the diffusion of the proteins from the bulk into the pure solvent region can be calculated analytically and added to the time-dependent adsorption that we calculate. However, the time scale of this process is so fast, compared to the processes calculated here, that its inclusion does not change any of the behavior presented.

An experimentally measurable quantity that we can calculate at equilibrium and as a function of time is the surface tension. The thermodynamic potential that we use in deriving the theory is exactly the free energy per unit area that corresponds to the surface tension (Rowlinson and Widom, 1982) when the bulk value is subtracted. We use the same excess free energy to calculate the dynamic surface tension. This is given (for both equilibrium and dynamic surface tension), by Eq. 1, which, for the binary mixture just presented, becomes

$$\beta\Pi(t) = \int_0^\infty \left[(\rho_1^{pro}(z; t) - \rho_{1,bulk}^{pro}) + (\rho_2^{pro}(z; t) - \rho_{2,bulk}^{pro}) \right.$$

$$\left. + \left(\frac{\phi_s(z; t)}{v_s} - \frac{\phi_{s,bulk}}{v_s} \right) + (\beta\pi(z; t) - \beta\pi_{bulk}) \right] dz, \quad (22)$$

where the values at equilibrium ($t \to \infty$) provide the thermodynamic surface tension.

The second system on which we report calculations is aimed at looking at the effect that surface-induced conformational transitions of the protein have on the equilibrium and kinetic process of adsorption.

The bulk solution is composed by spherical model proteins with a radius $R = 15$ Å, which interact with the surface with the potential shown in Fig. 3. Upon contact with the surface, the protein may undergo a conformational change to a configuration that we call pancake. This conformation has the shape of a disk with a height equal to ⅖ the diameter of the spherical conformation. The cross-sectional area of the disk is such that the volume of the protein is the same in the spherical and in the pancake configurations. The attraction of the pancake conformation with the surface is larger than that of the sphere. The motivation for studying this case is that, if the pancake conformation would not be more favorable on the surface, there will be no reason for the protein to undergo the conformational change upon contact with the surface. It is important to note that this type of configurational change, from a sphere-like conformation to
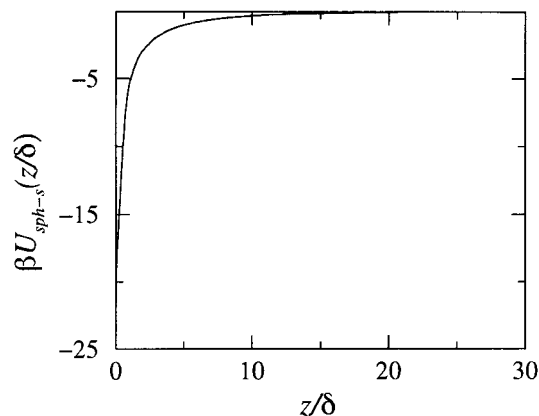

FIGURE 3 The distance dependence of the attractive interaction between the surface and one spherical protein for the case of proteins that may undergo conformational changes upon contact with the surface. Units are as in Fig. 2.

a more disk-like one, can be related to the conformational changes observed experimentally in studies of lysozyme adsorption (Billsten et al., 1995).

As in the case of the binary mixture, we assume that $\chi_{\gamma_i\gamma_j} = 0$ for all $\gamma_i\gamma_j$. Further, because there is only one relevant energy difference, we can take $U_{int}(\gamma_i) = 0$. Recall that the protein is allowed to change its configuration only at $z = 0$. The difference $U_{sph-s}(0) - U_{pan-s}(0)$ contains in it any difference in the internal energy between the two configurations.

The equations that are solved for the equilibrium system are

$$\rho_{sph}(z)v_s = \exp[\beta\mu_{bulk}^{pro}]\exp\left[-\beta U_{sph-s}(z) \right.$$

$$\left. - \int_z^{z+2R} \beta\pi(z')v_{sph}(z, z') \, dz' \right], \quad (23)$$

for all z, and there is an additional equation for the pancake conformation,

$$\rho_{pan}(0)v_s = \exp[\beta\mu_{bulk}^{pro}]\exp\left[-\beta U_{pan-s}(0) \right.$$

$$\left. - \int_0^h \beta\pi(z)v_{pan}(z) \, dz \right], \quad (24)$$

where $U_{pan-s}(0)$ is the pancake–surface attraction. The equation for the density of pancake conformations is only at $z = 0$ because this configuration is assumed to exist only upon contact of the protein with the surface.

The constraint equations to determine the lateral pressures for $z \leq h$ are

$$\rho_{\text{pan}}(0)v_{\text{pan}}(z) + \int_0^z \rho_{\text{sph}}(z')v_{\text{sph}}(z', z)\, dz' + \phi_s(z) = 1, \quad (25)$$

and, for $z > h$,

$$\int_{z-2R}^z \rho_{\text{sph}}(z')v_{\text{sph}}(z', z)\, dz' + \phi_s(z) = 1. \quad (26)$$

Again, as described above, these equations are solved by discretization of the z direction.

The kinetic equations for the sphere configuration are, for $z \neq 0$,

$$\frac{\partial \rho_{\text{sph}}(z, t)}{\partial t} = D_{\text{sph}} \frac{\partial}{\partial z}\left[\rho_{\text{sph}}(z; t)\frac{\partial \beta\mu_{\text{sph}}(z; t)}{\partial z}\right], \quad (27)$$

and, for $z = 0$,

$$\frac{\partial \rho_{\text{sph}}(0, t)}{\partial t} = D_{\text{sph}} \frac{\partial}{\partial z}\left[\rho_{\text{sph}}(0; t)\frac{\partial \beta\mu_{\text{sph}}(0; t)}{\partial z}\right]$$

$$+ k(\text{pan} \rightarrow \text{sph})\Phi(\text{pan} \rightarrow \text{sph}; t)\rho_{\text{pan}}(0; t)$$

$$- k(\text{sph} \rightarrow \text{pan})\Phi(\text{sph} \rightarrow \text{pan}; t)\rho_{\text{sph}}(0; t), \quad (28)$$

with the time-dependent chemical potential of the sphere given by

$$\beta\mu_{\text{sph}}(z; t) = \ln[\rho_{\text{sph}}(z; t)v_s] + \beta U_{\text{ps}}(z)$$

$$+ \int_z^{z+2R} \beta\pi(z'; t)v_{\text{sph}}(z, z')\, dz'. \quad (29)$$

The dynamic equation for the pancake configuration contains no mass transport component because it can only exist on the surface and as a transformation from an already adsorbed spherical conformation. Thus, we have

$$\frac{\partial \rho_{\text{pan}}(0; t)}{\partial t} = -k(\text{pan} \rightarrow \text{sph})\Phi(\text{pan} \rightarrow \text{sph}; t)\rho_{\text{pan}}(0; t)$$

$$+ k(\text{sph} \rightarrow \text{pan})\Phi(\text{sph} \rightarrow \text{pan}; t)\rho_{\text{sph}}(0; t), \quad (30)$$

where for both Eqs. 28 and 30, the blocking functions, are given by

$$\Phi(\text{pan} \rightarrow \text{sph}; t) = \exp[\beta(U_{\text{rep}}(\text{pan}; t) - U_{\text{rep}}(\text{sph}; t))], \quad (31)$$

with the repulsive contribution to the potentials of mean force given by

$$U_{\text{rep}}(\text{pan}; t) = \int_0^h \pi(z; t)v_{\text{pan}}(z)\, dz, \quad (32)$$

for the pancake, and

$$U_{\text{rep}}(\text{sph}; t) = \int_0^{2R} \pi(z; t)v_{\text{sph}}(z)\, dz, \quad (33)$$

for the sphere, where R is the radius of the spherical protein.

The intrinsic rates of conformational change, $k(\text{pan} \rightarrow \text{sph})$ and $k(\text{sph} \rightarrow \text{pan})$ are input for the theory. However, due to the condition of thermodynamic equilibrium, we only need to provide one. The equilibrium condition from which the constant is determined is

$$\frac{\rho_{\text{pan}}(0, \text{equil})}{\rho_{\text{sph}}(0, \text{equil})} = \frac{k(\text{sph} \rightarrow \text{pan})\Phi(\text{sph} \rightarrow \text{pan}; \text{equil})}{k(\text{pan} \rightarrow \text{sph})\Phi(\text{pan} \rightarrow \text{sph}; \text{equil})}, \quad (34)$$

where the equilibrium values of the densities and potentials of mean force for the blocking functions are determined from the equilibrium lateral pressures and chemical potentials as shown above (see Eqs. 23–26). In the results presented below, we provide, as input, $k(\text{sph} \rightarrow \text{pan})$.

Numerical methodology

The equilibrium equations require the discretization of space in the z direction. The way these equations are solved has been presented in detail in Szleifer (1997b). For clarity, we just mention some of the most important points. We discretize z into layers of thickness $\delta = D/5$, where D is the diameter of the largest protein that we model. This particular choice of the discretization has been shown to provide excellent results for the solution of the equilibrium equations (Szleifer, 1997b; McPherson et al., 1998; Satulovsky et al., 2000). Further, changes in the value of δ does not change any of the results presented throughout this paper. δ is the unit length used throughout.

With this discretization, we call layer i as the region between $(i - 1)\delta \leq z < i\delta$. Thus, all the integrations along z are transformed into sums over i. The next step is to determine the volume that a protein at layer k contributes to layer j. We consider a protein at layer k as the particle that has its point of closest approach to the surface at $(k - 1)\delta$. Then the volume that it occupies at layer j depends upon the geometry of the protein, as described in the Model Systems section. For example, for a spherical protein with $D = 5\delta$ the volumes are $v_p(1)/v_s = v_p(5)/v_s = 23.5488$; $v_p(2)/v_s = v_p(4)/v_s = 56.1547$; and $v_p(3)/v_s = 67.0234$. The unit volume used in all the calculation is the volume of the solvent, which is taken as $v_s = \delta^3/1.86^2$.

To exemplify a case of what the discrete equations that we solve for the equilibrium adsorption look like, we show

the example of a single type of spherical protein of diameter $D = 5\delta$ that is in solution with chemical potential μ_{p}. The discrete equations are

$$\sum_{k=1}^{5}\left\{[\rho^{\mathrm{pro}}(j - k + 1)v_{\mathrm{s}}]\left(\frac{v_{\mathrm{p}}(k)}{v_{\mathrm{s}}}\right)\right\} + \exp[-\beta\pi(j)v_{\mathrm{s}}] = 1$$

$$1 \leq j \leq j_{\max}, \quad (35)$$

where

$$\rho^{\mathrm{pro}}(i)v_{\mathrm{s}} = \exp\left[\beta\mu_{\mathrm{p}} - \beta U_{\mathrm{ps}}(i) - \sum_{l=1}^{5}[\pi(i + l - 1)v_{\mathrm{s}}]\right.$$

$$\left. \times \left(\frac{v_{\mathrm{p}}(l)}{v_{\mathrm{s}}}\right)\right], \quad (36)$$

where $U_{\mathrm{ps}}(i)$ is the strength of the protein–surface interaction at distance $(i - 1)\delta$ from the surface. $\rho^{\mathrm{pro}}(i)v_{\mathrm{s}}$ is the dimensionless density that we use throughout the Results section. In particular, what we call $\rho(0)$ in all the figures refers to $\rho^{\mathrm{pro}}(0)v_{\mathrm{s}}$.

Eqs. 35, with Eq. 36, represent a set of $j_{\max}$-coupled nonlinear equations for the $\pi(j)$ that are solved by numerical iterative methods (IMSL, 1989, Press et al., 1990). In most applications, we use $j_{\max} = 30$. In practice, it is actually more convenient to solve for $x(j) = \exp[-\beta\pi(j)v_{\mathrm{s}}]$. The reason being that $\beta\pi(j)v_{\mathrm{s}}$ is a positive quantity, and, therefore, $x(j)$ is bound between 0 and 1. The explicit set of equations that we solve are

$$\sum_{k=1}^{5}\left\{\exp[\beta\mu_{\mathrm{p}} - \beta U_{\mathrm{ps}}(j - k + 1)]\prod_{l=1}^{5}[x(j - k\right.$$

$$\left. + l)]^{v_{\mathrm{p}}(l)/v_{\mathrm{s}}}\frac{v_{\mathrm{p}}(k)}{v_{\mathrm{s}}}\right\} + x(j) = 1 \quad 1 \leq j \leq j_{\max}. \quad (37)$$

For the dynamic calculations, we can solve the kinetic equations, Eq. 19 and its analogs, Eqs. 27 and 28, by discretizing space as explained for the equilibrium equations and finite difference for the time domain. Namely, we calculate the rhs of the kinetic equations at time t and use it to solve for the values at the next time $t + \Delta t$.

For example, Eq. 19, for layer j, using finite differences for the time derivative, becomes

$$\frac{\rho_{\mathrm{i}}^{\mathrm{pro}}(j, t + \Delta t) - \rho_{\mathrm{i}}^{\mathrm{pro}}(j, t)}{\Delta t} = f(t), \quad (38)$$

with

$$f(t) = D_{\mathrm{i}}\left[\frac{\rho_{\mathrm{i}}^{\mathrm{pro}}(j + 1, t) - \rho_{\mathrm{i}}^{\mathrm{pro}}(j, t)}{\delta}\right]$$

$$\times \left[\frac{\mu_{\mathrm{i}}^{\mathrm{pro}}(j + 1, t) - \mu_{\mathrm{i}}^{\mathrm{pro}}(j, t)}{\delta}\right] + D_{\mathrm{i}}\rho_{\mathrm{i}}^{\mathrm{pro}}(j, t)$$

$$\times \left[\frac{\mu_{\mathrm{i}}^{\mathrm{pro}}(j + 1, t) - \mu_{\mathrm{i}}^{\mathrm{pro}}(j, t)}{\delta^2}\right] \quad j = 1; \quad (39)$$

and

$$f(t) = D_{\mathrm{i}}\left[\frac{\rho_{\mathrm{i}}^{\mathrm{pro}}(j + 1, t) - \rho_{\mathrm{i}}^{\mathrm{pro}}(j, t)}{\delta}\right]\left[\right.$$

$$\times \left.\frac{\mu_{\mathrm{i}}^{\mathrm{pro}}(j + 1, t) - \mu_{\mathrm{i}}^{\mathrm{pro}}(j, t)}{\delta}\right] + D_{\mathrm{i}}\rho_{\mathrm{i}}^{\mathrm{pro}}(j, t)$$

$$\times \left[\frac{\mu_{\mathrm{i}}^{\mathrm{pro}}(j + 1, t) - 2\mu_{\mathrm{i}}^{\mathrm{pro}}(j, t) + \mu_{\mathrm{i}}^{\mathrm{pro}}(j - 1, t)}{\delta^2}\right] \quad j > 1,$$

$$(40)$$

where we have used the dimensionless $\mu_{\mathrm{i}}^{\mathrm{pro}}$ and $\rho_{\mathrm{i}}^{\mathrm{pro}}$. Namely, $\mu_{\mathrm{i}}^{\mathrm{pro}} = \beta\mu_{\mathrm{i}}^{\mathrm{pro}}$, $\rho_{\mathrm{i}}^{\mathrm{pro}} = \rho_{\mathrm{i}}^{\mathrm{pro}}v_{\mathrm{s}}$. The chemical potentials are given by the discrete versions of Eq. 20. In this explicit way of solving the dynamic equations, all the values at time t are known. Using Eq. 38, we obtain $\rho_{\mathrm{i}}^{\mathrm{pro}}(z, t + \Delta t)$. The most important issue to consider now is how to choose the proper Δt so that the integration is correct.

Under optimal conditions, one would like to choose a very small time step Δt so that the finite difference is as close as possible to the derivative. However, if Δt is too small, it will take a long time to integrate the equations up to the new equilibrium state. Note that, in some cases, we integrate the equations of motion over many orders of magnitude in time. Thus, the proper balance needs to be found when choosing a good Δt. The way we obtain the optimal Δt is by an adaptive method that is schematically shown in Fig. 4. The basic idea is to attempt to integrate with the largest possible time step for which the integration is correct. We found that the particular choice of the increment of Δt shown in the figure enables the integration of the equations of motion in a reasonable amount of computer time for our calculations.

Using this procedure and its straightforward generalization for the case of conformational changes, we calculated all the dynamic results presented in this report. It should be stressed that we have not attempted to optimize the method to achieve optimal computational performance. Our main concern in all the calculations was the correct integration of the equation of motions in a reasonable amount of computer time. Future work, including proteins and polymers at surfaces, may require the optimization of the methodology, because the integration will need to be carried out over many more orders of magnitude in time, as a recent example shows (Satulovsky et al., 2000).

RESULTS

Thermodynamic behavior

We first present the results of the calculations for the equilibrium adsorption isotherms. For the binary mixture,
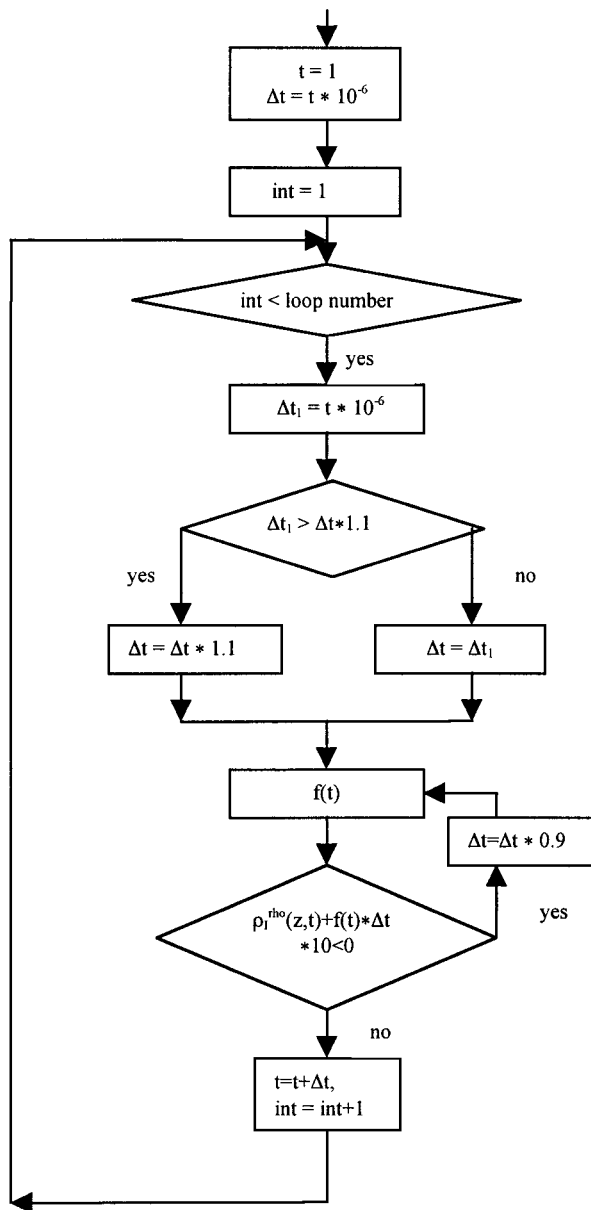
FIGURE 4 Flowchart representing the adaptive method used in the dynamic simulations.
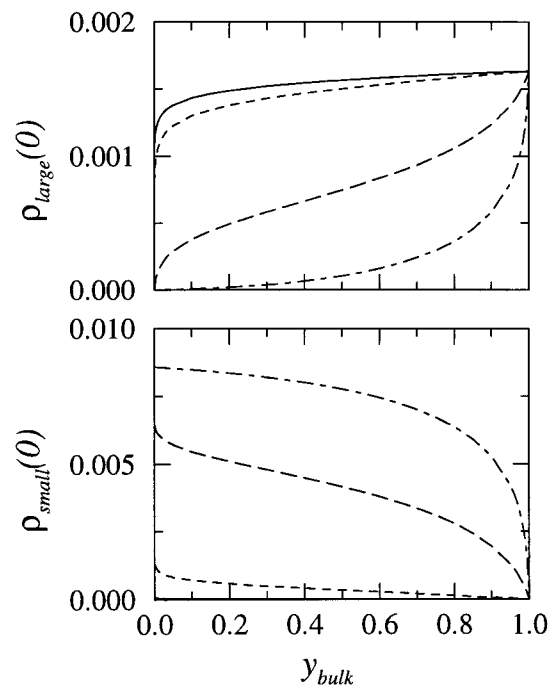

FIGURE 5 The equilibrium amount of large and small proteins adsorbed as a function of the mole fraction of the large protein in bulk. The different curves in each graph represent different ratios of $U_{\mathrm{ps}}^{\mathrm{large}}/U_{\mathrm{ps}}^{\mathrm{small}}$, for fixed large protein–surface attraction. $U_{\mathrm{ps}}^{\mathrm{large}}$ is as shown in Fig. 2. The different ratios are: *solid line*, $U_{\mathrm{ps}}^{\mathrm{large}}/U_{\mathrm{ps}}^{\mathrm{small}} = 5$; *dashed line*, $U_{\mathrm{ps}}^{\mathrm{large}}/U_{\mathrm{ps}}^{\mathrm{small}} = 3$; *long-dashed line*, $U_{\mathrm{ps}}^{\mathrm{large}}/U_{\mathrm{ps}}^{\mathrm{small}} = 2$; *dot-dashed line*, $U_{\mathrm{ps}}^{\mathrm{large}}/U_{\mathrm{ps}}^{\mathrm{small}} = 1.67$.

Fig. 5 shows the equilibrium amount of large and small proteins adsorbed as a function of the bulk composition of the mixture. The different curves in each graph represent different ratios of the strength of the protein–surface attraction for the small protein, for fixed attraction of the large one. The lowest ratio is 1.67, which is exactly the ratio of the radii of the proteins. The reason for considering this particular ratio is that, if the surface–protein attraction were dominated by van der Walls interactions, then the strength of these interactions is proportional to the radius of the particle (Israelachvili, 1991). For this case, even though the attraction is stronger for the large protein, the smaller pro-

teins adsorb in much larger amounts for all compositions. This shows the dominant effect of the repulsive interactions in determining the amount of protein adsorbed for this particular mixture.

Decrease of the strength of the small protein–surface attraction (increase of the ratio) results in an increase of the amount of large proteins adsorbed at the expense of the small ones. Note, however, that the change in the number of large proteins adsorbed going from a ratio of 3 to 5 is not very large. The main effect is to replace small proteins. This effect is best seen by showing the adsorption isotherm of the mixture in the form of surface mole fraction against the bulk mole fraction. This is shown in Fig. 6. For a ratio of attractive interactions of the order 2.5 and larger, the surface is dominated by the attractive strength of the large protein.

It is clear that the amount of protein adsorbed at equilibrium is the result of the balance between three competing thermodynamic forces. There is the bare surface–protein attraction that will favor the largest proteins. There is the entropy of mixing that will favor an equimolar mixture (this is not a major contribution but it cannot be neglected). The last contribution is the repulsive interactions between the adsorbed proteins. The larger proteins feel a stronger repulsive interaction upon contact with the surface due to their larger volume. These three contributions are further con-
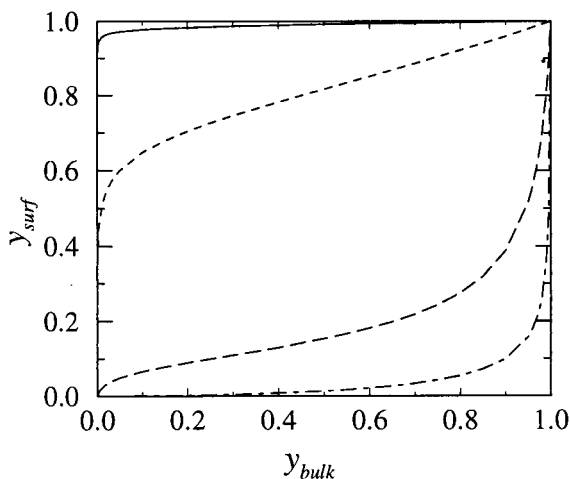
FIGURE 6 The surface mole fraction of the large protein as a function of the bulk mole fraction of the large protein. The different curves are as in Fig. 5.
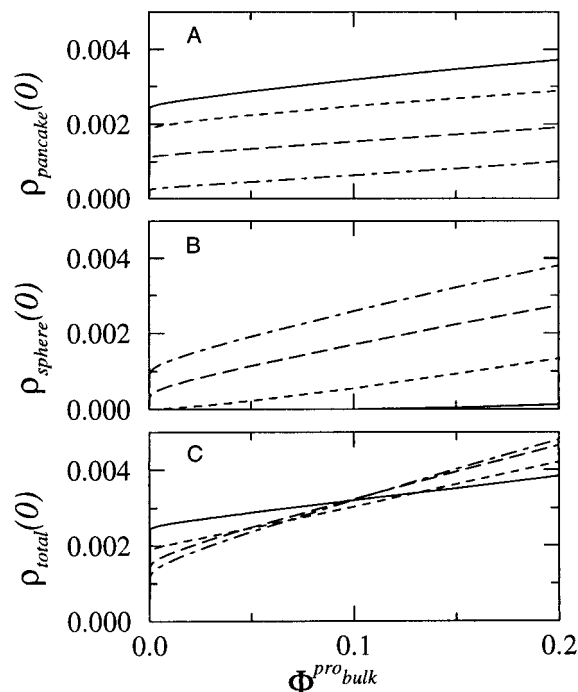

FIGURE 7 The equilibrium density of adsorbed sphere, pancake, and total (sphere + pancake) as a function of the bulk concentration of proteins for four different strengths of the pancake–surface interaction. In all cases, the sphere–surface attraction is fixed and as shown in Fig. 3. The four different pancake–surface interactions are: *solid line*, $U_{\text{pan-s}}(0) = 4U_{\text{sph-s}}(0)$; *dashed line*, $U_{\text{pan-s}}(0) = 3U_{\text{sph-s}}(0)$; *long-dashed line*, $U_{\text{pan-s}}(0) = 2U_{\text{sph-s}}(0)$; and *dot-dashed line*, $U_{\text{pan-s}}(0) = 1U_{\text{sph-s}}(0)$.

strained to the need to have the protein chemical potential on the surface equal to that in the bulk. Figures 5 and 6 show examples in which each of the different contributions dominate the adsorption. The isotherms can be used to design the proper surface chemistry to tune the protein–surface interaction, and the compositions that are optimal for preferential equilibrium adsorption of small or large proteins.

We now turn to the equilibrium adsorption isotherm of the protein that may undergo a conformational change upon adsorption on the surface. Figure 7 shows the density of sphere and pancake conformations adsorbed as a function of the bulk concentration of proteins for 4 different strengths of the pancake–surface interaction. As the attraction between the pancake and the surface increases, there is a larger number of pancake configurations on the surface. Note, however, that the slope of increase of the pancake configuration as a function of the bulk concentration of proteins is smaller than that of the spherical conformation. Therefore, as shown in Fig. 7 *C*, the total number of adsorbed proteins is not always larger when the pancake–surface attraction is maximal. Recall that all these calculations are for fixed sphere–surface interaction. At very low bulk concentrations of proteins, the maximal number of proteins on the surface corresponds to the case of maximal pancake–surface attraction. As the concentration of bulk protein increases, the amount of adsorbed proteins increases in all cases. However, the rate of increase of adsorbed proteins with bulk concentration is larger for the smallest pancake–surface attraction. The reason is that the pancake configuration has a much stronger repulsive component because most of its volume is localized in the close vicinity of the surface. (A schematic representation of the different repulsions in the pancake versus the spherical configuration is presented in Fig. 8.) The sphere conformation has the strongest repul-

sions at a distance R from the surface, which is larger than the thickness of the pancake. Further, due to the volume distribution in the sphere, the repulsive interactions are smaller than for the pancake. Thus, as the concentration increases, the sphere becomes more favorable than the pancake, even though the latter has a stronger bare surface–protein attraction.

An easy way to visualize the strength of the repulsive interactions is by considering only the adsorbed molecules at the surface and looking at the excluded volume of each of the conformations. As can be seen from Fig. 8, the pancake has a much larger excluded area than the sphere. Further,

FIGURE 8 Schematic representation of the relevant repulsive interactions for the pancake and spherical configurations. The pancake has the strongest repulsion in the close vicinity of the surface. The sphere conformation has the strongest repulsions at a distance R from the surface, which is larger than the thickness of the pancake (R is the radius of the spherical configuration).

the relevant excluded area of the spherical configuration with respect to the pancake is smaller than that with respect to the sphere. This is because the cross-sectional area of the sphere interacting with the pancake is at a distance from the surface that is smaller than the sphere radius.

From the examples on the binary mixture and the conformational preferential adsorption, we see that it is very important to include the strength of the surface–protein attraction and the intermolecular repulsions. Further, the repulsions depend very strongly on the shape and size of the molecules, and, therefore, a proper treatment of the equilibrium adsorption isotherms requires a theoretical description that is able to include all these components at the molecular level. Thus, we expect the theory to provide accurate adsorption isotherms if explicit information on the size and shape of the adsorbing proteins is given as input, when they become available.

We now have an understanding of what is the optimal final amount of protein adsorbed. The next step is to study how the system can reach that condition. We now present results for the kinetics of protein adsorption for the different cases of interest.

Kinetic adsorption

We start the discussion of the time-dependent adsorption for the case of mixtures. There is clear experimental evidence that, in the adsorption of blood proteins, there is exchange. In some cases, the smallest protein adsorbs first and, later, it is replaced by a larger protein. This kind of sequential adsorption is called the Vroman sequence (Green et al., 1999). We have seen that, from the equilibrium point of view, the optimal partition of the proteins on the surface depends upon the size of the particles, the bulk composition, and the surface–protein interaction. We expect these variables to be also important for the kinetic sequence, and we present the most representative results now. For all the mixtures that we show below, we consider the ratio of the diffusion coefficients to be inversely proportional to the ratio of the radius of the spheres. Namely, we use the Stokes–Einstein relation between the diffusion constant and the radius and assume that the viscosity coefficient is constant at all compositions.

Before we present the results, it is important to remember what is the initial condition in our system. In our kinetic studies, we assume that, at time $t = 0$ in the vicinity of the surface, the solvent molecules are homogeneously distributed at all $z(z < 6D_{large})$ and the density of the protein is very small. Further, we assume that, at a distance $z \geq 6D_{large}$, the composition does not change with time. In other words, at that distance, it is assumed that the proteins are always at their bulk composition. This is aimed to represent experiments of adsorption where the bulk solution is driven by a flow cell. Clearly, the distance from the surface where the density is constant is not known, and our choice is based

only on computational convenience. However, moving that distance to larger values will have an effect only on the diffusion-controlled regime of the kinetics. Recall the definition of the different kinetic regimes defined following Eq. 15. We believe that the qualitative features that we present below will not change. Only the time at which the kinetic-controlled regime stars will be modified. However, because the most interesting part is in the kinetic-controlled regime, and also the diffusion controlled-regime could be added analytically, we have chosen to keep the distance fixed at this relatively small value.

Figure 9 shows the time-dependent adsorption for each of the two proteins and the total amount of protein on the surface for three different bulk compositions for the largest attraction difference between the two proteins that we studied in the equilibrium case. For an equimolar solution, the kinetics show that the two proteins start to adsorb together. After a relatively short time, the small proteins' rate of adsorption decreases while that of the large protein continues to increase. The initial increase in the amount of small proteins adsorbed is because there is plenty of free surface accessible to the proteins. Once there are enough large proteins to exert a significant repulsive interaction on the
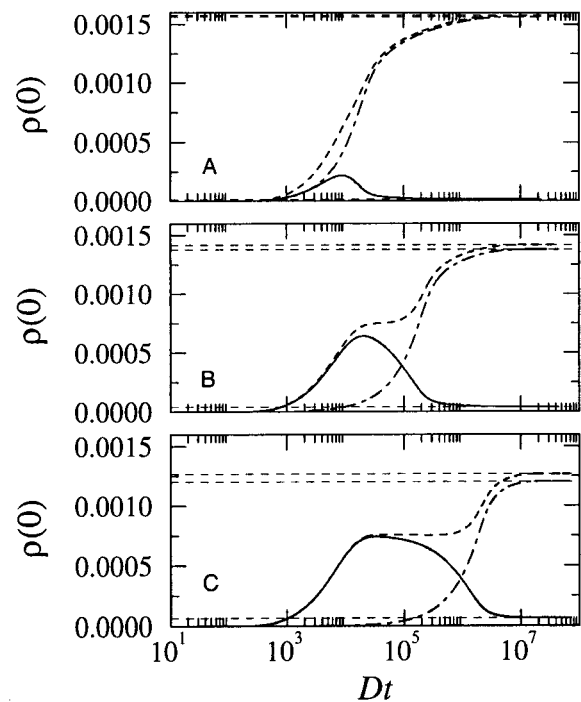

FIGURE 9 The time-dependent adsorption of large (*dot-dashed line*) and small (*solid line*) proteins on the surface for three different bulk composition and for $U_{ps}^{large}/U_{ps}^{small} = 5$. The total density of adsorbed proteins is represented by the dashed line. The bulk compositions are: (*A*) $y = 0.5$; (*B*) $y = 0.05$; (*C*) $y = 0.005$, where y is defined as the mole fraction of the large proteins in bulk. The time is measured in units of the diffusion coefficient of the small protein, D, $D = \frac{5}{3}D_{large}$. The time axis is in a logarithmic scale.

small proteins, the smaller particles start to desorb. For this equimolar mixture, there are plenty of large proteins close to the surface to adsorb at the initial steps of the adsorption process. Thus, there is no real competitive adsorption, but, essentially, free adsorption of the two different proteins until the repulsive interactions are strong enough that there is no gain for the small proteins to reach or stay on the surface. Recall that the large protein–surface attraction is rather large.

The other two bulk compositions show a rather different kinetic behavior. Namely, there is an initial large adsorption of the small particles before the large proteins start to adsorb and displace the small ones. This is the result of the smaller number of large proteins in the bulk solution, and, thus, there is a delay for the larger particles to reach the surface. These cases are in line with the experimentally observed Vroman sequence. Thus, we conclude that, to observe the Vroman sequence, the necessary conditions are that the bulk solution is at a composition with an excess of the small protein, and that the interaction between the large protein and the surface is much larger than that of the smaller protein.

The question that arises is what is the driving force for the desorption of the small proteins. Recall that, in our theoretical approach, the desorption is not added as a term in a kinetic equation, but, if observed, it is the result of the competing interactions that determine the dynamic path. The motion of the proteins is driven by the gradient in chemical potential. The chemical potential has three contributions (see Eq. 20). The contribution of the surface–protein attraction to the gradient of chemical potential is independent of time, and it is at all times the driving forces for the proteins to go to the surface. The desorption is the result of the other two contributions and the changes in these quantities when the large proteins start to adsorb on the surface. It turns out that the repulsive potential of mean force is relatively small in magnitude compared to the other contributions under these conditions. The term arising from the ideal translational entropy is large. This term, which by itself will tend to drive the motion to have a uniform density profile (maximal entropy), acts in opposite direction to the attractive interaction term.

To see the differences with single-protein adsorption and to understand the origin of the desorption process in mixtures, we show, in Fig. 10, the adsorption of a single protein from solution. In this case, the amount of protein at the surface as a function of time is monotonic (as shown in Fig. 10 *A*). The rate of adsorption is not monotonic, and, as is shown in Fig. 10 *B*, it has a very fast regime at short times. The fast regime is dominated by the time that it takes the proteins to reach a distance of the order of the protein diameter from the surface. At this distance, the strength of the attractive interaction is very large and thus the surface acts as a sink. Note that this will be the case only for dilute
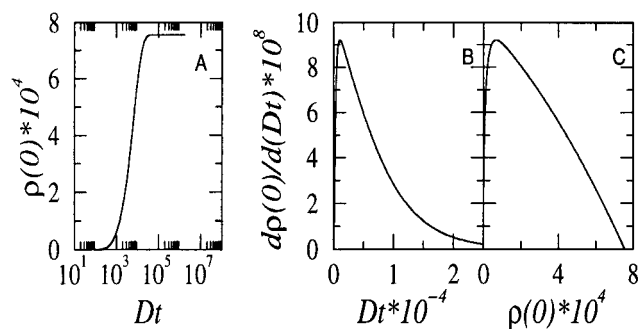

FIGURE 10 The time-dependent adsorption of pure small proteins. (*A*) Density of proteins adsorbed on the surface as a function of time; (*B*) the rate of adsorption as a function of time; (*C*) the rate of adsorption as a function of the density of adsorbed proteins. The time is measured in units of the diffusion coefficient of the protein, *D*. The time axis in Panel A is in a logarithmic scale.

surfaces, so that there are no repulsive interactions acting on the system.

As proteins adsorb, the repulsive term due to the already adsorbed proteins becomes more important, and there is a maximum in the rate followed by a long tail of decreasing rate as the repulsions become more and more dominant. The rate, however, remains positive at all times. This is the same behavior as has been recently observed experimentally by C. Calonder and P. R. Van Tassel (2001) for the adsorption of human fibronectin.

In the case of mixtures, as shown in Fig. 9, at the beginning of the adsorption process, the adsorbing small proteins do not feel at all the presence of the large ones, and, thus, the adsorption rate and total adsorption is very similar to that of the single small protein in solution, shown in Fig. 10. However, as the large proteins start to adsorb, the environment for the small ones changes completely as compared to the single-component case. We find that the main change that drives the desorption is the result of the pushing of the small proteins that are close to the surface but not yet adsorbed by the large adsorbed proteins. This results in a relatively large gradient of the density of small proteins that drives the small adsorbed proteins out of the surface.

An interesting aspect of the different kinetic behavior observed for the different compositions can be obtained by looking at the total surface density (adsorption) as a function of time. This is shown in Fig. 11, together with the change in the dynamic surface tension for the three cases. We see that, in the case where the large proteins replace the adsorbed small ones, the total adsorption shows a plateau region. This is also observed in the dynamic surface tension. The duration of the plateau depends upon the rate of exchange between the large and the small proteins. Note that, in both cases, the plateau is at exactly the same total density, and also total lateral pressure.

The results presented in Fig. 11 suggest that experimental observations of the dynamic surface tension in protein mix-
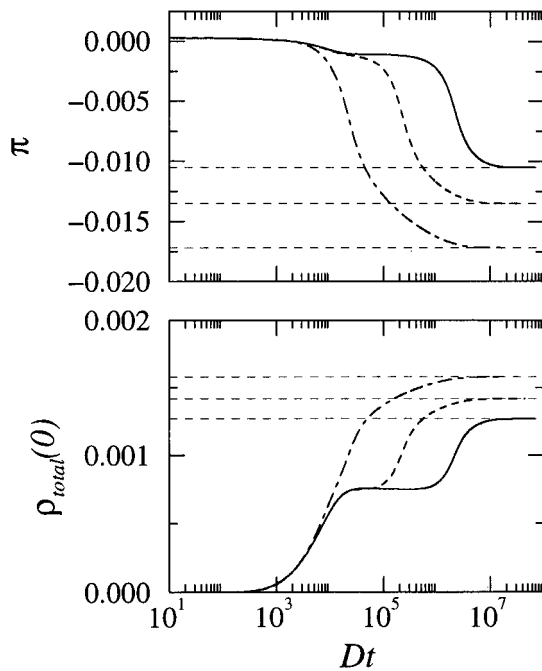
FIGURE 11   The dynamic surface tension as a function of time (*top*) and the total amount of proteins adsorbed as a function of time (*bottom*) for three different bulk compositions of mixtures of proteins. *Solid line*, $y = 0.005$; *dashed line*, $y = 0.05$; and *dot-dashed line*, $y = 0.5$. The time is measured in units of the diffusion coefficient of the small protein, D. The time axis is in a logarithmic scale.
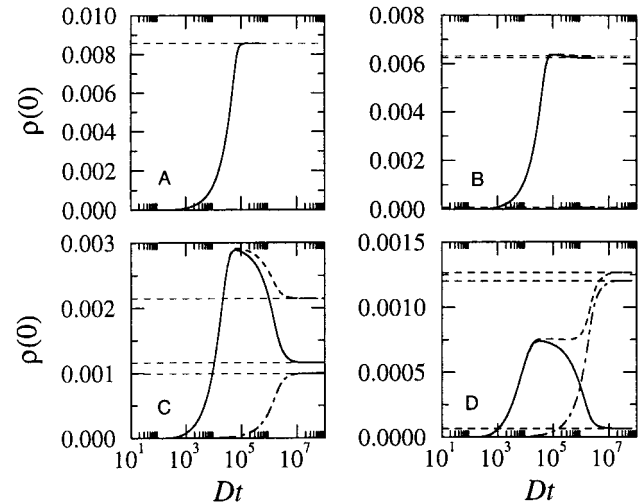

FIGURE 12   The time-dependent adsorption of large (*dot-dashed line*), small (*solid line*), and the total amount (*dashed line*) of proteins on the surface, for fixed bulk composition ($y = 0.005$) and four different ratios of strength of protein–surface attractions between large and small proteins: (*A*) $U_{ps}^{large}/U_{ps}^{small} = 1.67$; (*B*) $U_{ps}^{large}/U_{ps}^{small} = 2$; (*C*) $U_{ps}^{large}/U_{ps}^{small} = 3$; and (*D*) $U_{ps}^{large}/U_{ps}^{small} = 5$. The time is measured in units of the diffusion coefficient of the small protein, D. The time axis is in a logarithmic scale.

tures should be interpreted with special care. In particular, it is clear that the presence of a constant surface tension over a relatively long time is not necessarily an indication of the system reaching thermodynamic equilibrium. Our calculations suggest that a way to check whether constant surface tension indicates equilibrium is to carry out the experiments at a different bulk composition. The reason being that the equilibrium surface tension depends upon the composition, whereas the plateau is independent of the bulk value and it is the same for all compositions. The value of the plateau seems to depend only upon the kinds of proteins in the mixture and the protein–surface interactions.

The next question that we address is the effect of the strength of the protein–surface interactions on the kinetics of adsorption. Figure 12 shows the amount of protein adsorbed as a function of time for four different strengths of the small protein–surface attraction. The different interactions are as those used in the equilibrium calculations shown in Fig. 5. For the largest attraction for the small protein, there is almost no large protein adsorption. The time-dependent adsorption looks very similar to that of the pure small protein (Fig. 10). The reason is that, under these conditions, there is a very small amount of large proteins reaching the surface both in the equilibrium structure and on the kinetic pathway. As the interaction of the small protein decreases, there is a more important presence of the large protein at

equilibrium and in the kinetic adsorption. In all cases there is a much larger concentration of small particles in the bulk solution, and, thus, they adsorb first at a fast rate. Only after the large proteins start reaching the surface do the small proteins start to desorb to leave enough room on the surface for the large proteins. Note that, even though, in all cases, there is an overshoot of the small proteins on the surface at intermediate times, only at the smallest surface–small protein interactions does one see the typical Vroman sequence that results in more large proteins adsorbed at the end of the process.

The results presented in Fig. 12 show that one could control the temporary composition of proteins on the surface by controlling the flow of proteins and the surface–protein interactions. Furthermore, surface modification can lead to yet another degree of freedom to control the equilibrium and kinetic composition of the adsorbed layer.

A detail understanding of the different stages of adsorption for both types of proteins can be obtained by looking at the potential of mean force (see Eq. 10). Figure 13 shows the average potential felt by the large and small proteins at two different times in the adsorption process, for the cases shown in Fig. 12, *C* and *D*. For the case with the smallest strength of interaction between the small protein and the surface, the potentials of mean force at relatively short times looks very similar to the bare surface–protein interaction. This is basically the diffusion-controlled regime where the driving force for adsorption is just the strong protein–surface attraction. The potentials for the latter time show a qualitative different behavior. For both the small and large
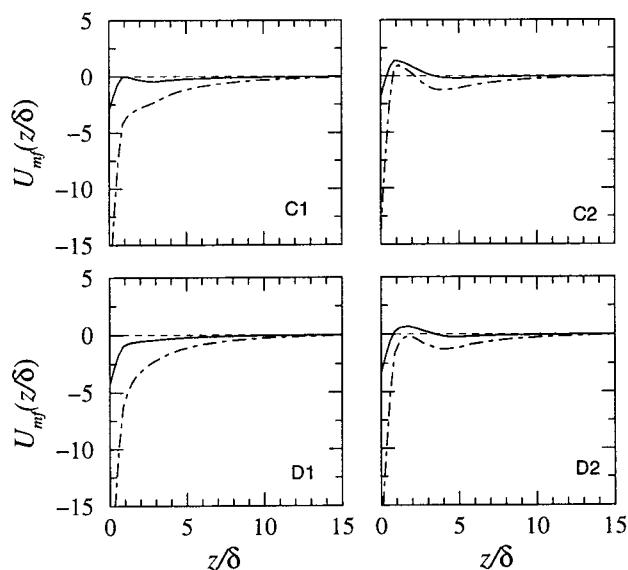
FIGURE 13 The potential of mean force felt by the large (*dot-dashed line*) and small (*solid line*) proteins at two different times in the adsorption process. (*C1*) and (*C2*) correspond to the case shown in Fig. 12 *C*, and (*D1*) and (*D2*) correspond to the case shown in Fig. 12 *D*. (*C1*) and (*D1*) correspond to time $Dt = 22025$, and (*C2*) and (*D2*) correspond to time $Dt = 1202541$. The time is measured in units of the diffusion coefficient of the small protein, D. The dashed line corresponds to zero potential.

proteins, there is a maximum in the potential of interaction. For the smallest protein, this is a repulsive maximum that makes the dynamic process to be now kinetically controlled. The time-dependent behavior is dominated by the time scale of crossing the barrier. Note that, even for the large protein, the approach to the surface requires a "jump" over a maximum in the potential. The position of the maxima in the potential corresponds to the size of the small proteins, and its presence reflects the repulsive interactions that the already adsorbed small proteins present to the proteins attempting to reach the surface from the solution.

The shape of the repulsive potential reflects the molecular structure of the adsorbed proteins and their organization on the surface. This can be seen in the cases shown in Fig. 13 *C*, where the barriers are more pronounced due to the larger density of molecules already adsorb at the times shown. In all cases, the presence of the barriers due to the already adsorbed (mostly small) proteins makes for the slow kinetics of the system to achieve final equilibrium. The shape and size of the potential of mean force is seen to change with time. This has two very important consequences. The first is that the type of kinetic process that determines the adsorption depends upon the molecular organization of the proteins close to the surface and the specific properties of the adsorbing proteins. Second, it demonstrates why the kinetics of protein adsorption is not a simple kinetic process, since the effective size and shape of the protein–surface potential changes as a function of time.

We now turn to the problem of the kinetics of adsorption on systems that the proteins may undergo conformational changes upon adsorption on the surface. We will consider solutions with a single kind of protein that, upon adsorption, can transform from its spherical conformation to the pancake. We have shown in Fig. 7 what is the partition between the two configurations at equilibrium. How the system reaches that equilibrium depends upon the rate of change from one conformation to the other. Inspection of Eq. 28 shows that there are two factors that determine the rate of change from the sphere to the pancake configuration. The first is the intrinsic rate of change $k(\text{sph} \to \text{pan})$, which measures the rate of conformational transformation for the isolated molecule. The second is the factor that depends upon the environment on the surface, $\Phi(\text{sph} \to \text{pan}; t)$. From these two factors, only the first one can be changed a priori to check the effect of different intrinsic rates on the kinetics of adsorption. The effect of the environment depends on the time evolution of the density of the different species on the surface, and, thus, it is, in essence, the result of how the system evolves in time.

Figure 14 shows the adsorption as a function of time for four different values of the intrinsic rate of change from the sphere to the pancake. The change in rate results in dramatic changes in the qualitative shape of the adsorption curves. For very fast intrinsic rates of transformation from sphere to pancake, the proteins change their configuration in a time scale faster than they are adsorbed. Thus, up to $Dt = 10^4$, there are only pancake configurations on the surface. Recall
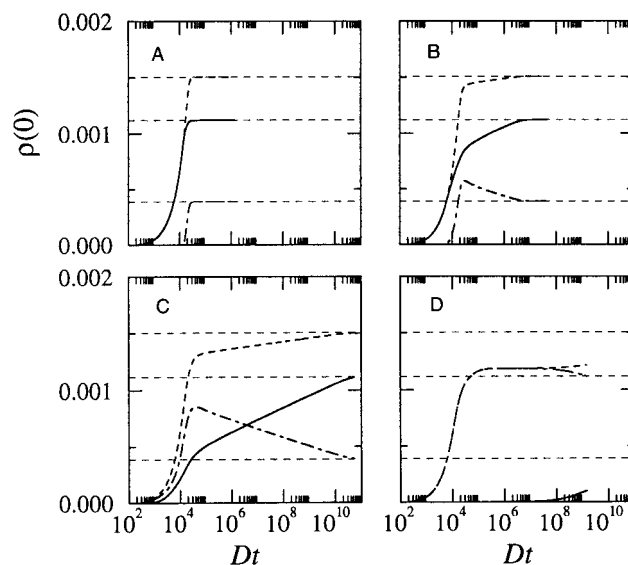

FIGURE 14 The time-dependent adsorption of sphere (*dot-dashed line*), pancake (*solid line*), and their sum (*dashed line*) for four different values of the intrinsic rate of conformational change from sphere to pancake. (*A*) $k_{sp}^{int}/D = 4.85 * 10^4$; (*B*) $k_{sp}^{int}/D = 4.85 * 10^0$; (*C*) $k_{sp}^{int}/D = 4.85 * 10^{-4}$; and (*D*) $k_{sp}^{int}/D = 4.85 * 10^{-12}$. D is the diffusion coefficient of the spherical proteins. The time axis is in a logarithmic scale.

that the pancake has a much stronger attraction with the surface than does the sphere. At this time there is a large enough concentration of proteins adsorbed (all in pancake configuration) that the rate of transformation from sphere to pancake decreases dramatically due to the excluded volume term. Namely, the pancake requires more free space on the surface than does the sphere. Thus, the relatively high density on the surface prevents the fast transformation, and, thus, the spheres' density starts to increase up to the point that the system reaches equilibrium with the ratio of sphere to pancakes that minimizes the free energy.

When the rate $k(\text{sph} \rightarrow \text{pan})$ is decreased by four orders of magnitude (Fig. 14 *B*), it can be seen that the beginning of the adsorption process is very similar to the faster one (Fig. 14 *A*). However, once the density on the surface is large enough for the excluded volume term to become relevant, the compound rate of transformation is slow enough that there is an overshoot on the adsorption of the spherical configuration that decays over two orders of magnitude in time until the system reaches thermodynamic equilibrium. Note that the time to reach equilibrium is two orders of magnitude slower than that in the case shown in Fig. 14 *A*.

A further decrease of the bare rate constant makes the diffusion of the particles to the surface much faster than the transformation to pancake. Thus, as can be seen in Fig. 14 *C*, the beginning of the adsorption process changes as compared to the faster ones, because the number of spherical proteins is larger than those of pancake for a very long period of time. Actually, the number of pancake configuration becomes equal to that of spheres only after $Dt = 10^6$, which corresponds to a time longer than what the systems in Fig. 14, *A* and *B*, take to reach thermodynamic equilibrium.

Figure 14 *D* shows the adsorption in the case of a very low value for the rate constant $k(\text{sph} \rightarrow \text{pan})$. As can be seen up to $Dt = 10^8$, the system behaves as if there are only spherical proteins. Our calculation did not reach equilibrium, and we believe that the system is several orders of magnitudes off equilibrium. The reason that we show this example is that it represents an interesting case where the system shows indications of irreversible behavior, even though the formulation of the theory is such that the systems eventually will reach thermodynamic equilibrium. An interesting result of this behavior is shown in Fig. 15, where the dynamic surface tension is shown as a function of time for the same cases shown in Fig. 14. The initial fast decrease of the dynamic surface tension is determined by the diffusion-controlled regime of the adsorption, namely, the time that it takes the particles to diffuse to the surface. If the rate of transformation to pancake is fast enough, then there is no change in the curvature of the dynamic surface tension. However, once the rate of transformation is small enough that the lateral repulsive interactions play a role, there is a slowdown on the decrease of the dynamic surface tension. In the limiting case of very slow transformation, we see a
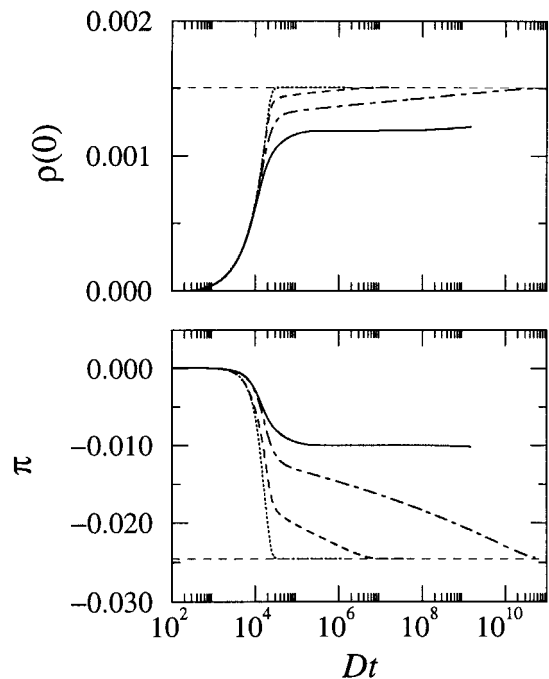

FIGURE 15 The total amount of protein adsorbed (*upper graph*) and the dynamic surface tension (*lower graph*) as a function of time for four different values of the intrinsic rate of change from sphere to pancake. *Dotted line*, $k_{sp}^{int}/D = 4.85 * 10^4$; *dashed line*, $k_{sp}^{int}/D = 4.85 * 10^0$; *dot-dashed line*, $k_{sp}^{int}/D = 4.85 * 10^{-4}$; and *solid line*, $k_{sp}^{int}/D = 4.85 * 10^{-12}$. The time is measured in units of the diffusion coefficient of the spherical proteins, D. The time axis is in a logarithmic scale.

plateau that may be confused with the system reaching thermodynamic equilibrium.

The results of Fig. 15 are interesting because they show that measurements of the dynamic surface tension may provide indications that the proteins undergo conformational changes upon adsorption. This is particularly evident in the case of relatively slow rate of conformational change, but fast enough that the system reaches equilibrium in a reasonable amount of time.

The total rate of conformational change, and, thus, the time that it takes the system to reach equilibrium, is determined by two factors. The first is the absolute rate of conformational transition, and it is independent of the state of the surface. The second is the effect of the surface density, and it measures the repulsive interactions difference between the two configurations and the neighboring molecules. This second factor is a strong function of the surface density and composition and it varies with time. This is the term that is responsible for the sharp slowdown and for the change in the rate of adsorption. To visualize this effect, Fig. 16 shows the variation of the repulsive term as a function of time for the four cases shown in Fig. 14. The figure clearly demonstrates the decrease by more than five orders of magnitude in the rate due to the repulsive interactions. It is interesting to note that, as the population of
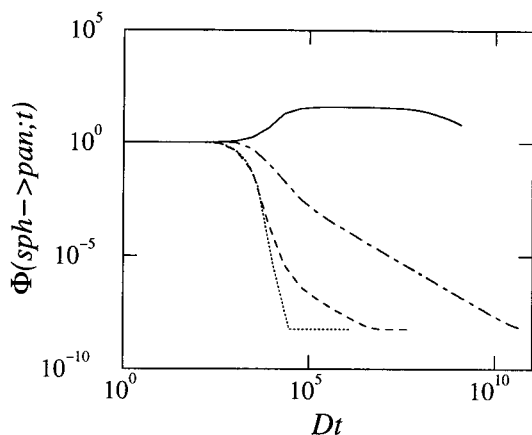
FIGURE 16 The variation of the blocking function as a function of time for the four cases shown in Fig. 15. The time is measured in units of the diffusion coefficient of the spherical proteins, D. The time axis is in a logarithmic scale.

pancake on the surface increases, there is a very sharp decrease of the rate. This is because the pancake conformation occupies more surface area than does the sphere.

CONCLUSIONS

We have presented a general theoretical approach to study the thermodynamic and kinetic behavior of adsorbing proteins on solid surfaces. We have derived the theory in its most general form for both the equilibrium and kinetic studies. The theory was then applied to simple cases to study the effect of size, composition, surface–protein interactions, and protein conformational changes to the adsorption isotherms and the kinetics of protein adsorption.

The formulation of the theory does not require the specific introduction of the kinetic pathways that may happen through the adsorption process, but it predicts them. For example, adsorption and desorption will be predicted if the local thermodynamic environment is optimal for that process. Further, the kinetic version of the theory is formulated such that the system will eventually reach thermodynamic equilibrium. However, the theory is capable of predicting some kind of irreversible adsorption for cases of very slow dynamic processes. The theory describes the adsorption process from the bulk solution to the surface, including a detailed description of the region in the vicinity of the surface. Further, although the theory was presented here assuming that the only inhomogeneous direction is that perpendicular to the surface, it can be easily extended to treat inhomogeneous three-dimensional systems (Seok et al. 2000). The theory enables the study of the changes of the structure of the adsorbed layer, with molecular detail, as a function of time. This molecular description allows the understanding of the factors that determine the different kinetic regimes.

The theory requires, as input, the intermolecular and surface–protein interactions, and the possible conformations of the proteins. The intrinsic rate of transformation from one conformation to another also needs to be given. These are very difficult quantities to obtain, and, therefore, we applied the theory to simple systems to study the main factors determining the adsorption behavior. Although the application of the theory was done for simple geometries for the proteins, the real configuration of the protein could be included if they are known. As more microscopic understanding of the structure and conformational properties of proteins are learned, they can be incorporated into the theoretical framework. Actually, the lack of knowledge of the conformational properties of proteins may be one of the most important limitations in the application of the theory.

The complete understanding of the adsorption process should optimally permit description of the dynamic changes from the nanosecond time scale, which is the time scale for local conformational changes, to hours, which is the time scale of the whole adsorption process. Clearly, this is an impossible computational task with current methodologies and hardware. Note that atomistic simulations can be run for a single solvated small protein for nanoseconds. The theory presented here is aimed at bridging the gap between microseconds and hours. We hope, in the future, to be able to introduce the input necessary for the theory from molecular dynamic simulations of single proteins and, thus, bridge the gap between the atomistic time scale to the macroscopic one. It is important to emphasize that, to describe the very large range of time scales that the theory can treat, one needs to compromise in atomistic detail. Thus, the description of the solvent and basic elements forming the proteins are coarse grained. The level of coarse graining depends upon the level of detail that is of interest and the time scale of the overall process.

It is important also to emphasize the limitations of the approach presented here. First, although the theory has shown the ability to quantitatively predict the adsorption isotherms of lysozyme and fibrinogen on hydrophobic surfaces with grafted PEO (McPherson. et al., 1998; Satulovsky et al., 2000), it is still a mean-field theory with all its limitations, in particular with respect to the lateral interactions. The applicability of the theory can be improved by considering inhomogeneous densities in all three dimensions, (see, e.g., Seok et al., 2000). However, even though some correlations will be accounted for, the theory will remain, in essence, a mean-field approach. Second, for the kinetic behavior, we have assumed that the diffusion in the plane of the surface is much faster than the motion perpendicular to it. Although Brownian Dynamics simulations (Ravichandran and Talbot, 2000) show that this is a valid approximation for layers that are not very dense, we cannot predict a priori whether this is going to be the case generally. Again, this limitation may partially be overcome by considering the motion in all three directions. However, this

will require an extremely large computational effort. Third, the theory requires, as input, the information on the molecular details of the proteins. This information has to be coarse grained to be able to integrate the equations of motion. Therefore, some of the detailed structural information is lost. Fourth, the theory assumes that there is a separation of time scales between the diffusion of the proteins (slow motion) and the rearrangement of the solvent molecules (fast motion). Although this is generally a reasonable approximation, it may have important consequences, in particular regarding solvent rearrangements upon conformational changes of the protein. Atomistic studies of single proteins in solvents may shed light on the cases in which this approximation breaks down. Fifth, we have assumed that the diffusion constant of the protein does not change with composition. Further, the approach assumes that there are no flow effects.

The advantages of the theory, such as the ability to study kinetic processes over many orders of magnitude in time, the ability to follow the adsorption with a large degree of molecular detail, and the wide range of applicability of the approach, should be balanced against its limitations to apply this approach in the appropriate cases where the theory is valid. The conclusions presented here are kept within that context, and we believe that the generic behaviors that we have found are applicable in a large range of systems in which adsorption of proteins takes place.

We have found that the competitive adsorption of proteins from solution can show a variety of different behaviors depending upon the protein–surface interactions, the composition of the bulk solution, and the ratio of sizes between the proteins. We found, in agreement with experimental observations, that the Vroman sequence is obtained when the large proteins have a much stronger attractive interaction with the surface than the smaller ones and the bulk solution is rich in the small proteins. Changing the composition of the bulk solutions puts the large proteins at a larger concentration on the surface at all times. The results presented here show the different conditions under which one can temporarily and thermodynamically control the adsorption of proteins on surfaces. Thus, they can serve as one of the building blocks in the design of optimal surfaces for protein separations. Our findings on the plateau of the dynamic surface tension suggest that changing the bulk composition of the protein mixture may be a good indicator of whether the system has achieved thermodynamic equilibrium. The equilibrium value of the surface tension will depend upon bulk composition, whereas the dynamic plateau will not.

The ability of the protein molecules to change their conformation upon adsorption has dramatic effects on the kinetics of protein adsorption. Depending upon the intrinsic rate of conformational change compared to protein diffusion, one can observe different adsorption patterns that are determined also by the intermolecular interactions. These interactions, in turn, depend on the population of different conformers on the surface. Our findings suggest that measurements of dynamic surface tension versus time may give an indication of possible conformational changes upon adsorption. Slow conformational changes seem to be associated with changes in the slope of the dynamic surface tension versus time. Further, the intermolecular interactions play a key role in the rate of conformational transformation once a certain density threshold of proteins is found on the surface. These results may lead to ways of surface modification that can be used to selectively adsorb proteins in a given configuration.

To summarize, the work presented here is one more step toward the systematic understanding of the molecular factors that determine the adsorption of proteins on surfaces. The complexity in the dynamic and equilibrium behavior calculated even for our simple protein models are comparable to those observed experimentally. Further, it demonstrates that explicit incorporation of the size, shape, composition, and strength of the intermolecular and surface interactions are necessary for the proper description of these complex systems. For example, the complex and time-dependent shape of the potentials of mean force demonstrate that the kinetics of adsorption is a process associated with multiple relaxation times that are strongly dependent upon the size and shape of the molecules.

We are currently working on simple detailed models of proteins that will enable us to include more molecular and conformational detail as input to the theory. In parallel, we plan to compare the predictions of the theory with available experimental data to build up a database of useful models of proteins with which the theory can predict the behavior of real systems.

REFERENCES

Andrade, J. D., and V. Hlady. 1986. Protein adsorption and materials biocompatibility: a tutorial review and suggested hypotheses. *Adv. Polym. Sci.*, 79:1–63.

Billsten, P., M. Wahlgren, T. Arnebrant, J. Mcguire, and H. Elwing. 1995. Structural-changes of T4 lysozyme upon adsorption to silica nanoparticles measured by circular-dichroism. *J. Colloid Interface Sci.*, 175:77–82.

Brooks, C. L., III, M. Gruebele, J. N. Onuchic, and P. G. Wolynes. 1998. Chemical physics of protein folding. *Proc. Nat. Acad. Sci. U.S.A.*, 95:11037–11038.

Calondes, C., and P. R. Van Tassel. 2001. Kinetic regimes of protein adsorption. *Langmuir.* In press.

Carignano, M. A., and I. Szleifer. 1994. Structure and thermodynamics of grafted three-arm branched polymer layers. *Macromolecules.* 27:702–710.

Chan, H. S., and K. A. Dill. 1998. Protein folding in the landscape perspective: chevron plots and non-arrhenius kinetics. *Proteins Struct. Funct. Genet.* 30:2–33.

Chandler, D. 1987. Introduction to Modern Statistical Mechanics. Oxford University Press, New York. 188–229.

Chatelier, R. C., and A. P. Minton. 1996. Adsorption of globular proteins on locally planar surfaces: models for the effect of excluded surface area and aggregation of adsorbed protein on adsorption equilibria. *Biophys. J.* 71:2367–2374.

Cho, D., G. Narsimhan, and E. I. Franses. 1997. Adsorption dynamics of native and pentylated bovine serum albumin at air–water interfaces: surface concentration/surface pressure measurements. *J. Colloid Interface Sci.* 191:312–325.

Clerc, D., and W. Lukosz. 1997. Real-time analysis of avidin adsorption with an integrated-optical output grating coupler: adsorption kinetics and optical anisotropy of adsorbed monomolecular layers. *Biosens. Bioelectron.* 12:185–194.

Denizli, A., H. Yavuz, B. Garipcan, and M. Y. Arica. 2000. Nonporous monosize polymeric sorbents: dye and metal chelate affinity separation of lysozyme. *J. Appl. Polym. Sci.* 76:115–124.

Diamant, H., and D. Andelman. 1996. Kinetics of surfactant adsorption at fluid/fluid interfaces: non-ionic surfactants. *Europhys. Lett.* 34:575–580.

Luscher, E. F., and S. Weber. 1993. The formation of the haemostatic plug—a special case of platelet aggregation: an experiment and a survey of the literature. *Thromb. Haemostasis.* 70:234–237.

Feder, J., and I. Giaever. 1980. Adsorption of ferritin. *J. Colloid Interface Sci.* 78:144–154.

Fraaije, J. G. E. M. 1993. Dynamic density functional theory for microphase separation kinetics of block copolymer melts. *J. Chem. Phys.* 99:9202–9212.

Ghose, S., and H. Chase. 2000. Expanded bed chromatography of proteins in small diameter columns. I. Scale down and validation. *Bioseparation.* 9:21–28.

Gidalevitz, D., Z.-q. Huang, and S. A. Rice. 1999. Protein folding at the air–water interface studied with x-ray reflectivity. *Proc. Nat. Acad. Sci. U.S.A.* 96:2608–2611.

Green, R. J., M. C. Davies, C. J. Roberts, and S. J. B. Tendler. 1999. Competitive protein adsorption as observed by surface plasmon resonance. *Biomaterials.* 20:385–391.

Hasegawa, R., and M. Doi. 1997. Adsorption dynamics. Extension of self-consistent field theory to dynamical problems. *Macromolecules.* 30:3086–3089.

Hlady, V., and J. Buijs. 1996. Protein adsorption on solid surfaces. *Curr. Opin. Biotechnol.* 7:72–77.

Horbett, T. A. 1993. Principles underlying the role of adsorbed plasma proteins in blood interactions with foreign materials. *Cardiovasc. Pathol.* 2:137S–148S.

1989. USER'S MANUAL: IMSL MATH/LIBRARY, FORTRAN Subroutines for Mathematical Applications. 780.

Iordanskii, A. L., V. S. Markin, L. P. Razumovskii, R. Y. Kosenko, N. A. Tarasova, and G. E. Zaikov. 1996. Diffusion model of protein adsorption and effect of protein layer composition on water permeability for ultra-filtration membranes. *Desalination.* 104:113–118.

Ishihara, K., H. Nomura, T. Mihara, K. Kurita, Y. Iwasaki, and N. Nakabayashi. 1998. Why do phospholipid polymers reduce protein adsorption? *J. Biomed. Materials Res.* 39:323–330.

Israelachvili, J. 1991. Intermolecular and Surface Forces. Academic Press, London.

Kondo, A., and H. Fukuda. 1998. Effects of adsorption conditions on kinetics of protein adsorption and conformational changes at ultrafine silica particles. *J. Colloid Interface Sci.* 198:34–41.

Lassen, B., and M. Malmsten. 1997. Competitive protein adsorption at plasma polymer surface. *J. Colloid Interface Sci.* 186:9–16.

Lee, S. J., and K. Park. 1994. Protein interaction with surfaces: separation distance-dependent interaction energies. *J. Vac. Sci. Technol.* 12:1–7.

Malmsten, M. 1997. Ellipsometry and tirf studies of adsorption processes in parenteral drug delivery. *Interface Science.* 5:159–167.

Marconi, U. M. B., and P. Tarazona. 1999. Dynamic density functional theory of fluids. *J. Chem. Phys.* 110:8032–8044.

McPherson, T. A. Kidane, I. Szleifer, and K. Park. 1998. Prevention of protein adsorption by tethered poly(ethylene oxide) layers: experiments and single-chain mean-field analysis. *Langmuir.* 14:176–186.

Minton, A. P. 1999. Desorption of globular proteins on locally planar surfaces. II. Models for the effect of multiple adsorbate conformations on adsorption equilibria and kinetics. *Biophys. J.* 76:176–187.

Montdargent, B., and D. Letourneur. 2000. Toward new biomaterials. *Infect. Control Hosp. Epidemiol.* 21:404–410.

Nasir, A., and J. McGuire. 1998. Sequential and competitive adsorption of bovine serum albumin and beta-lactoglobulin, and their resistance to exchange with alpha-lactalbumin and beta-casein. *Food Hydrocoll.* 12:95–103.

Norde, W., and C. E. Giacomelli. 1999. Conformational changes in proteins at interfaces: from solution to the interface, and back. *Macromol. Symp.* 145:125–136.

Norde, W., and C. E. Giacomelli. 2000. BSA structural changes during homomolecular exchange between the adsorbed and the dissolved states. *J. Biotechnol.* 79:259–268.

Nyquist, R. M., A. S. Eberhardt, L. A. Silks, Z. Li, X. Yang, and B. I. Swanson. 2000. Characterization of self-assembled monolayers for biosensor applications. *Langmuir.* 16:1793–1800.

Olson, C. A., and J. Talbot. 2000. Equilibria and kinetics of polydisperse mixture adsorption. *J. Chem. Phys.* 112:3868–3874.

Press, H. W., P. B. Flannery, A. S. Teukolsky, and T. W. Vetterling. 1990. Numerical Recipes: The Art of Scientific Computing (Fortran Version). the Press Syndicate of the University of Cambridge.

Ravichandran, S., and J. Talbot. 2000. Mobility of adsorbed proteins: a Brownian dynamics study. *Biophys. J.* 78:110–120.

Rowlinson, J. S., and B. Widom. 1982. Molecular Theory of Capillarity. Clarendon Press, Oxford.

Satulovsky, J., M. A. Carignano, and I. Szleifer. 2000. Kinetic and thermodynamic control of protein adsorption. *Proc. Nat. Acad. Sci. U.S.A.* 97:9037–9041.

Schaaf, P., and J. Talbot. 1989. Surface exclusion effects in adsorption processes. *J. Chem. Phys.* 91:4401–4409.

Scheraga, H. A. 1996. Recent developments in the theory of protein folding: searching for the global energy minimum. *Biophys. Chem.* 59:329–339.

Seok, C., K. F. Freed, and I. Szleifer. 2000. Polymer melts and polymer solutions near patterned surfaces. *J. Chem. Phys.* 112:6443–6451.

Shi, H. Q., and B. D. Ratner. 2000. Template recognition of protein-imprinted polymer surfaces. *J. Biomed. Materials Res.* 49:1–11.

Slomkowski, S. 1998. Polyacrolein containing microspheres: synthesis, properties and possible medical applications. *Prog. Polym. Sci.* 23:815–874.

Slomkowski, S., M. Kowalczyk, M. Trznadel, and M. Kryszewski. 1996. Two-dimensional latex assemblies for biosensors. *Hydrogels Biodegrad. Polym. Bioappl.* 627:172–186.

Sukhishvili, S. A., and S. Granick. 1999. Adsorption of human serum albumin: dependence on molecular architecture of the oppositely charged surface. *J. Chem. Phys.* 110:10153–10161.

Szleifer, I. 1997a. Polymers and proteins: interactions at interfaces. *Curr. Opin. Solid State Mater. Sci.* 2:337–344.

Szleifer, I. 1997b. Protein adsorption on surface with grafted polymers: a theoretical approach. *Biophys. J.* 72:595–612.

Szleifer, I., and M. A. Carignano. 1996. Tethered polymer layers. *Adv. Chem. Phys.* 94:165–260.

Tan, J. S., and P. A. Martic. 1990. Protein adsorption and conformational change on small polymer particles. *J. Colloid Interface Sci.* 136:415–431.

Tanaka, M., T. Motomura, M. Kawada, T. Anzai, Y. Kasori, T. Shiroya, K. Shimura, M. Onishi, and A. Mochizuki. 2000. Blood compatible aspects of poly(2-methoxyethylacrylate) (PMEA)—relationship between protein adsorption and platelet adhesion on PMEA surface. *Biomaterials.* 21:1471–1481.

Topoglidis, E., A. E. G. Cass, G. Gilardi, S. Sadeghi, N. Beaumont, and J. R. Durrant. 1998. Protein adsorption on nanocrystalline TiO2 films: an

immobilization strategy for bioanalytical devices. *Analyt. Chem.* 70: 5111–5113.

Van Tassel, P. R., L. Guemouri, J. J. Ramsden, G. Tarjus, P. Viot, and J. Talbot. 1998. A particle-level model of irreversible protein adsorption with a postadsorption transition. *J. Colloid Interface Sci.* 207:317–323.

Van Tassel, P. R., J. Talbot, G. Tarjus, and P. Viot. 1996. Kinetics of irreversible adsorption with a particle conformational change: a density expansion approach. Part B. *Phys. Rev. E.* 53:785–798.

Van Tassel, P. R., P. Viot, G. Tarjus, and J. Talbot. 1994. Irreversible adsorption of macro-molecules at a liquid–solid interface—theoretical studies of the effects of conformational change. *J. Chem. Phys.* 101: 7064–7073.

Wang, N. H. L. 1993. Competitive protein adsorption in chromatography systems. *J. Cell. Biochem.* 17A:43–43, Suppl.

Yue, K., K. M. Fiebig, P. D. Thomas, H. S. Chan, E. I. Shakhnovich, and K. A. Dill. 1995. A test of lattice protein folding algorithms. *Proc. Nat. Acad. Sci. U.S.A.* 92:325–329.

Zhou, A. H., Q. J. Xie, P. Li, L. H. Nie, and S. Z. Yao. 2000. Piezoelectric crystal impedance analysis for investigating the modification processes of protein, cross-linker, and DNA on gold surface. *Appl. Surf. Sci.* 158:141–146.